1952

Engineering report on magnetic pulse formers and magnetic coincidence gates.

Kistler, W. C.

Monterey, California: U.S. Naval Postgraduate School

ENGINEERING REPORT ON MAGNETIC PULSE FORMERS AND MAGNETIC COINCIDENCE GATES

W. C. Kistler

Letter on front cover:

ENGINEERING REPORT ON MAGNETIC PULSE FORMERS AND MAGNETIC COINCIDENCE GATES

W. C. Kistler

LABORATORY REPORT NO. 1378

ENGINEERING REPORT ON MAGNETIC PULSE FORMERS AND MAGNETIC COINCIDENCE GATES

Submitted to the
United States Naval Postgraduate School
Monterey, California

FEDERAL TELECOMMUNICATION LABORATORIES, INC.
500 WASHINGTON AVENUE
NUTLEY 10, NEW JERSEY

COPY NO. 2

Prepared By: W. C. KISTLER, LT. U.S.N.

April 1952

LABORATORY REPORT NO. 1378

ENGINEERING REPORT ON MAGNETIC PULSE FORMERS AND MAGNETIC COINCIDENCE GATES

C O N T E N T S

ILLUSTRATIONS

FOREWORD

A brief explanation of the manner in which this report is written is considered necessary. The project reported on is a small integral portion of a jointly sponsored Bureau of Ships-Bureau of Aeronautics contract of classified nature. In order to avoid the complications of classifying the report, the name and designation of the over-all system have been omitted and only a few general details of its purpose and operation have been mentioned. This is considered jusitified since the problems attacked were not at all unique to the requirements of the equipment proposed by the contract, whose completion requires no new or unusual electronic concepts but only new and improved techniques of achieving the required characteristics of performance, reliability, and limitations of weight, space, and power.

Since the project undertaken was independent of the work being done on the remainder of the system, only work which was actually accomplished by the writer has been discussed. Some effort, less than ten per cent of the over-all total, was spent in joint analysis and development of instrumentation and other circuitry with company engineers. Because of its disconnected nature and lack of relation to the primary project, this work was not considered of sufficient interest to warrant interruption of the continuity of the report and therefore has not been included.

As is clarified in the main body of the report, the project consisted of two closely allied sections, but a decided emphasis of time and effort was devoted to one of the sections. Attention was given the other during periods when materials or test equipment were in the process of procurement or construction. Again in the interests of continuity, the two problems are treated separately in the report.

In view of the essential straightforwardness of the basic electron and electrical concepts involved, only a minimum of background material has been included in the report. The bibliography is believed to include in detail all such material which may be required for complete understanding of the report.

The successful completion of this project was achieved only as a result of the extremely helpful and friendly cooperation of my associates at the Federal Telecommunication Laboratories. Particular credit is due Mr. Ben Alexander and Mr. Robert C. Renick for their excellent technical advice and Miss Julie Yerzley and Mr. Paul E. Magdeburger for their generous assistance in preparing this report.

LABORATORY REPORT NO. 1378

ENGINEERING REPORT ON MAGNETIC PULSE FORMERS AND MAGNETIC COINCIDENCE GATES

I. INTRODUCTION

1. A pulse-time modulator currently under development at the Federal Telecommunication Laboratories requires the accurate generation of timing pulses from a reference and phase-shifted 2500-5000 cps sine wave.

2. A block diagram of such an equipment is shown in its simplest form in Figure 1. The phase-shift modulator may take any form provided its output is an undistorted sine wave of the same nature and amplitude as its input. The pulse formers must create a pulse of current or voltage from a sine-wave input; the pulse must possess a relatively steep leading edge and a nonvarying phase relationship with the input sine wave. For the desired application it was decided that the following specifications for the pulse formers should apply:

Pulse Amplitude	50 volts
Pulse Rise Time	1 microsecond
Position Accuracy	1/2 microsecond
Input Voltage	70 volts
Input Volt-Amperes	1 volt-ampere

SIMPLE PULSE TIME MODULATION SYSTEM

Figure 1

TOLERANCE	MATERIAL	TITLE			
UP TO 6 / ABOVE 6 TO 24 / ABOVE 24					
DEC. DIM. ±.005 / ±.010 / ±.015					
FRACT. DIM. ± 1/64 / ± 1/32 / ± 1/16	FINISH	ISSUED	USED WITH	AP'PD	DWN.
UNLESS OTHERWISE SPECIFIED					
Federal Telecommunication Laboratories, Inc.					-1

3. The above requirements may be fulfilled readily by conventional schemes employing vacuum tubes. Such a pulse former is shown in Figure 2 and will be discussed briefly later. The advantages of replacing this fairly involved circuit with one containing only passive elements are obvious. The most impressive gains would be in the areas of reliability and efficiency. A careful investigation into the possibility of designing and building a magnetic pulse former of suitable characteristics was considered highly desirable.

4. In order to improve the signal-to-noise ratio in the equipment mentioned previously, it is planned to employ a gating system which will eliminate all random noise except during a short interval in which the signal is expected to appear. Again conventional coincidence-type vacuum-tube circuits may be utilized, but a considerable improvement in reliability alone would be achieved if magnetic coincidence gates were substituted for their vacuum-tube counterparts.

5. Thus two related problems are presented, the investigation of magnetic pulse formers and magnetic coincidence gates. Emphasis has been given to the first problem because of its potentially greater importance and prior chronological position in the development of the system. Because of the relation of the two problems, the initial study of pertinent reference material and the subsequent analytical and experimental research on the characteristics and basic properties of the magnetic core materials available was so arranged that it could be utilized for both sections of the project. The work therefore consisted of three phases: (1) initial research; (2) pulse-former investigation; and (3) coincidence-gate investigation.

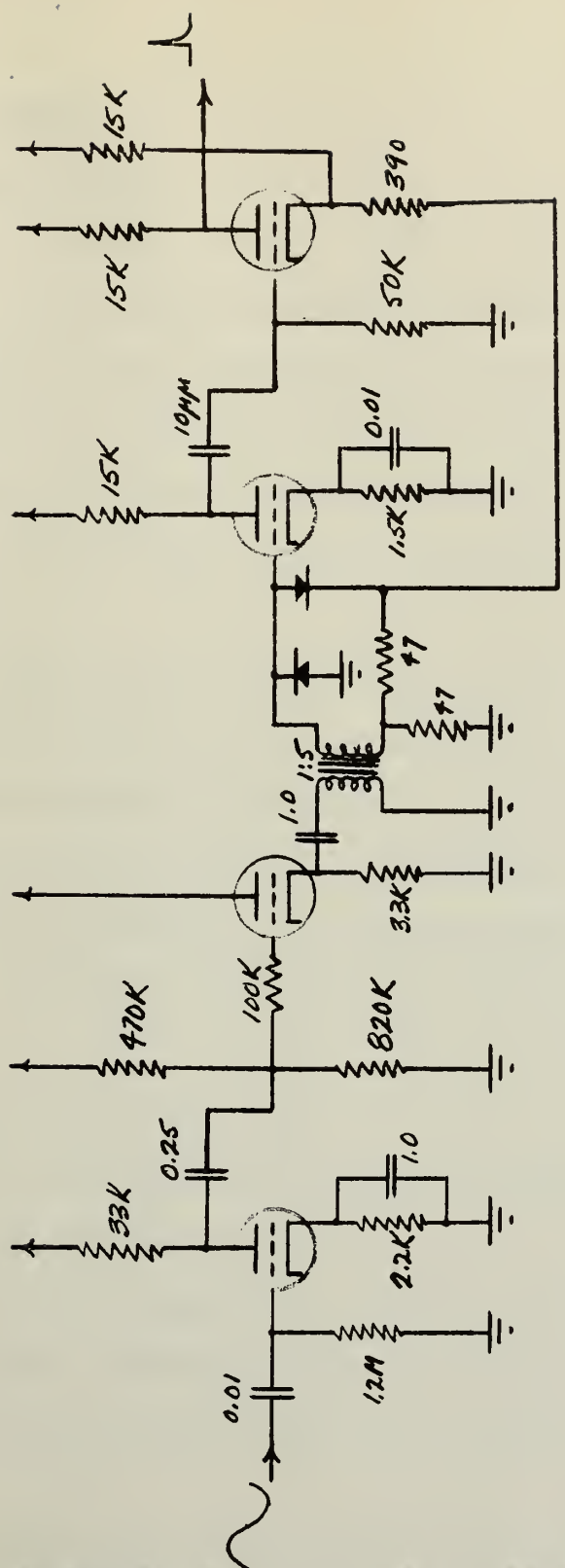

VACUUM TUBE PULSE FORMING CIRCUIT

Figure 2

TOLERANCE				MATERIAL	TITLE			
	UP TO 6	ABOVE 6 TO 24	ABOVE 24					
DEC. DIM.	±.005	±.010	±.015					
FRACT. DIM.	± 1/64	± 1/32	± 1/16	FINISH	ISSUED	USED WITH	AP'PD	DWN.
UNLESS OTHERWISE SPECIFIED								

Federal Telecommunication Laboratories, Inc. -1

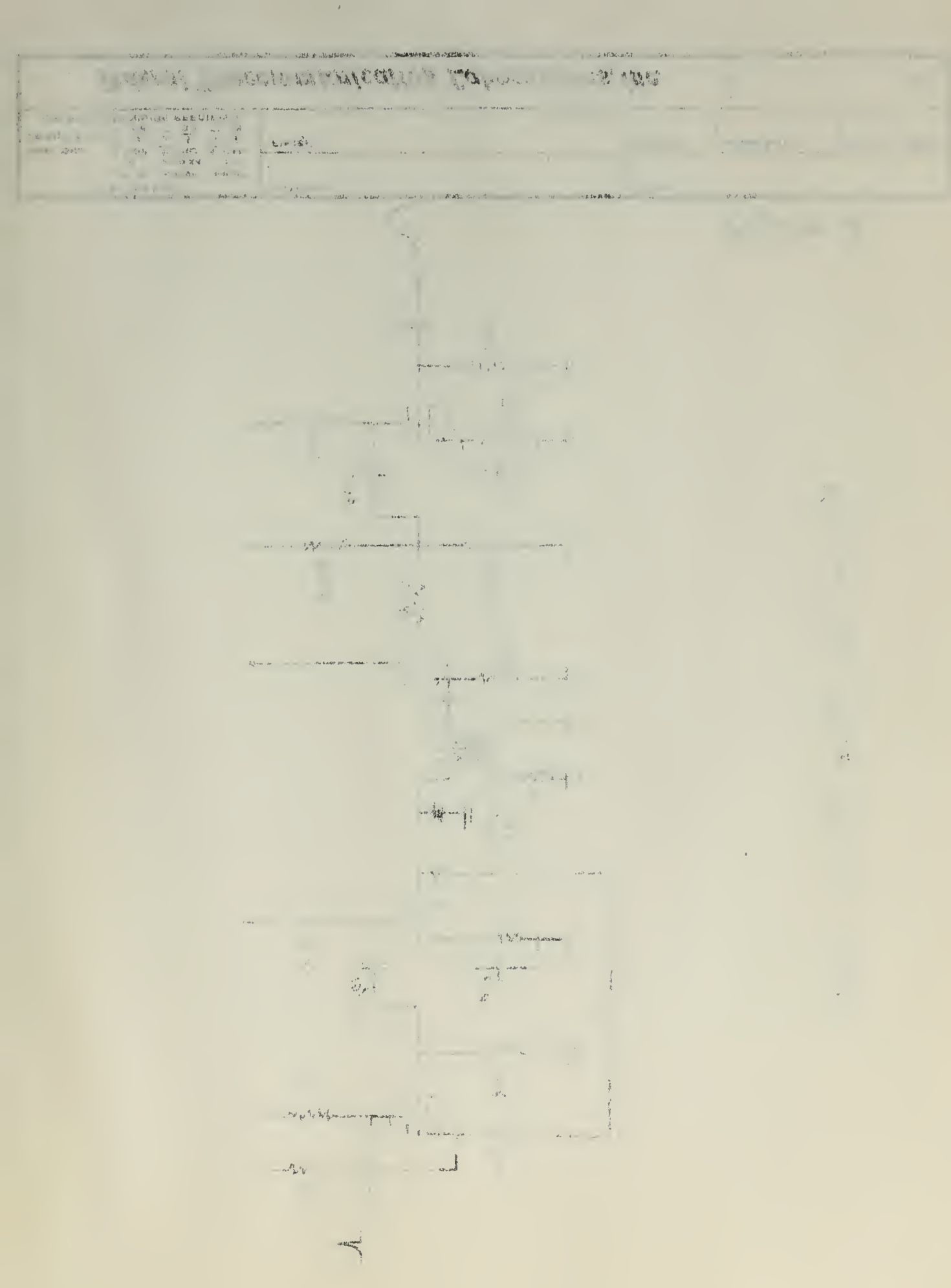

II. INITIAL RESEARCH

A. Core Materials

6. In order to contrive a magnetically-controlled system which will act as a pulse former or a coincidence gate, it is necessary to utilize a device commonly called a saturable-core reactor. The chief factors determining the performance of a saturable reactor are the magnetic characteristics of its core material. The general characteristics desired in a saturable-core reactor are, as will be shown later, low-saturation flux density and high incremental permeability.

7. Two distinct classes of magnetic materials exist, distinguished from each other both by their properties and their application. The classes may be called "permanent-magnet materials," which are of no particular interest in this application, and "magnetic core materials." The latter class may be further divided into metallic and nonmetallic groups.

8. The metallic core materials include the following five subgroups:

(1.) High purity iron

(2.) Iron-silicon alloys (0.5 to 5.0% Si)

(3.) Iron-nickel alloys

(4.) Iron-nickel alloys modified by the addition of small amounts of silicon, molybdenum, copper, or chromium

(5.) Iron-cobalt alloys with or without a third element such as vanadium.

9. Due to their relatively low saturation-flux densities, only the iron-nickel alloys of subgroups (3) and (4) warrant consideration. These alloys fall roughly into two general types, the 45-50% nickel alloys and the 75-80% nickel alloys. The other constituents are added to the basic composition

types to develop special properties, generally at the expense of reducing the fundamental properties of high permeability and low hysteresis losses.

10. For the first type, these alloys have been variously designated as Nicaloi (General Electric), Electric Metal (Allegheny Ludlum), Deltamax (Arnold Engineering), Hipernic (Westinghouse), and Carpenter "49" Alloy (Magnetic Metals). The second type has been given such names as Mumetal (Allegheny Ludlum), Mo-Permalloy and Supermalloy (Arnold Engineering), Carpenter Hymu "80" (Magnetic Metals), and Permalloy (Western Electric). Cores of both types, namely, Deltamax, Supermalloy, and Mo-Permalloy, were available for test purposes.

11. Deltamax, a grain-oriented 50% nickel-iron alloy having a rectangular hysteresis loop, finds wide use in magnetic amplifiers. Its properties are achieved by severe cold-reduction, and it is thus available only in the form of thin strip or tape. Mo-Permalloy consists of 79% nickel, 4% molybdenum, and 17% iron. It is produced in the form of cold-rolled strip by closely controlled melting, rolling, and heat-treating techniques but is not grain-oriented. Supermalloy, which is 79% nickel, 5% molybdenum, and 16% iron, is closely related to Mo-Permalloy in chemical composition but differs somewhat in basic magnetic properties due to different forming and heat-treating techniques. The latter materials display high permeabilities and low saturation-flux densities.

12. The cores are fabricated in toroidal form by continuously winding thin, insulated tape about a mandrel or core form. The tape has thicknesses of 1, 2, and 4 mils, but present developments indicate that 1/8-mil tape will soon be available.

13. The nonmetallic core materials are generally called ferromagnetics or ferrites. They are available under such names as Ferroxcube (Ferroxcube

Corp.) and Ferramics (General Ceramics). Because of their fairly high permeability and rapid response time due to negligible eddy-current losses, these materials are of particular interest in the coincidence-gate application.

14. The ferrites are a mixture of crystals of iron oxide with various other metallic oxides. Their general chemical formula is $XOFe_2O_6$, where X stands for a bivalent metal such as magnesium, nickel, or zinc. No metals in metallic form and no organic compounds are contained in the ferritic materials.

15. Perhaps the outstanding feature of ferrites is their extremely high volume resistivity. This keeps eddy-current losses to negligible values and so greatly improves the frequency-response characteristics of the core material. Other basic properties of ferritic materials are indicated by Figure 3, which shows B-H curves of a series of Ferramic materials. Types C, H, and J were available for test purposes.

B. Testing of Core Materials

16. The presently available engineering data on magnetic core materials provides information on their magnetic characteristics only at or below excitation frequencies of 400 cps. With the 2700-cps driving signal used in this application, the information which might be extrapolated from the published curves was not considered sufficiently reliable. An attempt to determine accurately the B-H curves (hysteresis loops) of the various core materials at 2700 cps was therefore decided upon.

17. The means employed to obtain a graphical presentation of the desired information is shown in Figure 4. That the horizontal deflection, D_h, is proportional to the magnetizing force, H, may be shown as follows (k_h is the horizontal deflection sensitivity of the CRO):

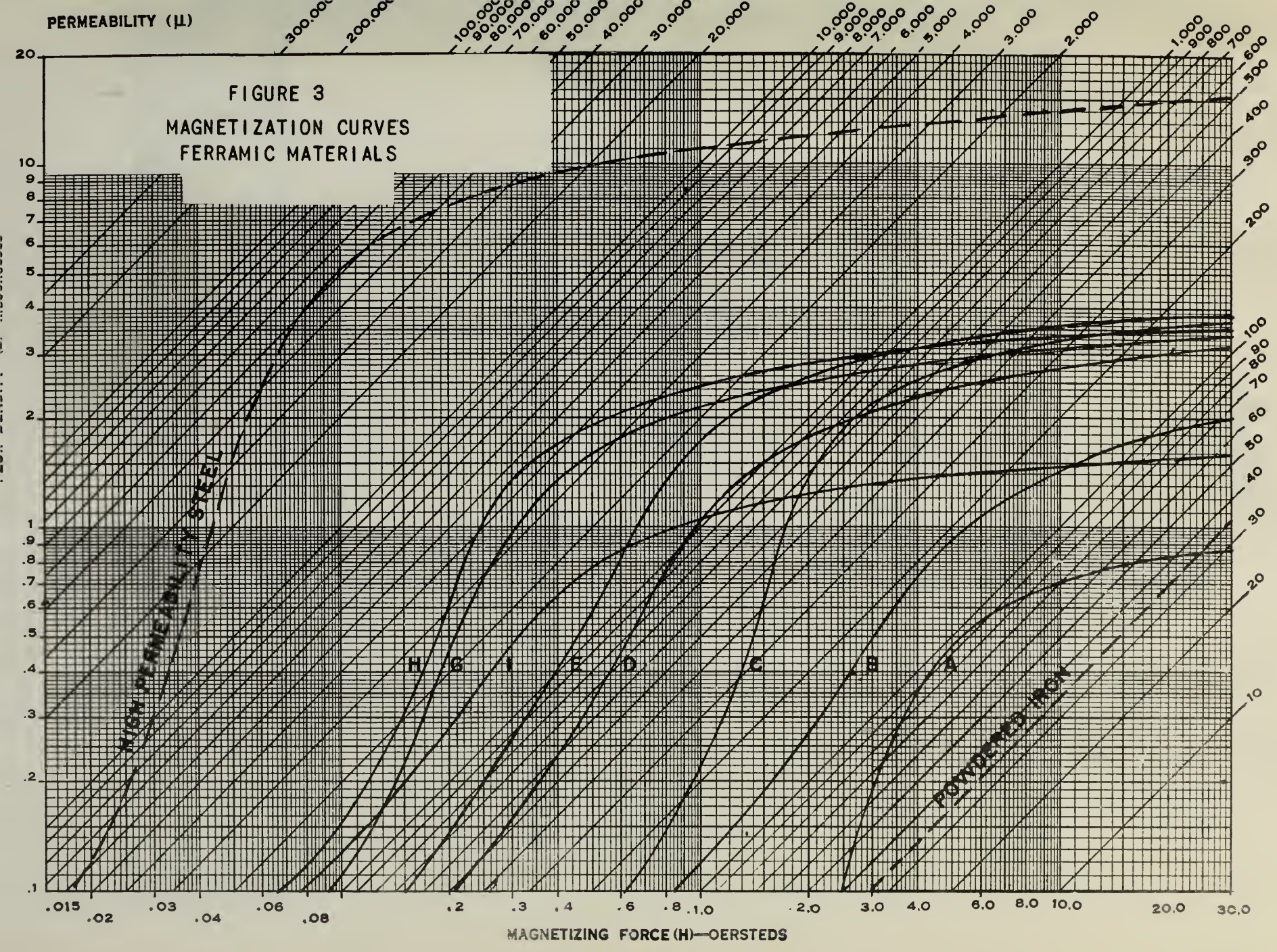
FIGURE 3
MAGNETIZATION CURVES
FERRAMIC MATERIALS
PERMEABILITY (μ)
MAGNETIZING FORCE (H)—OERSTEDS
HIGH PERMEABILITY STEEL
POWDERED IRON
A
B
C
D
E
F
G
H

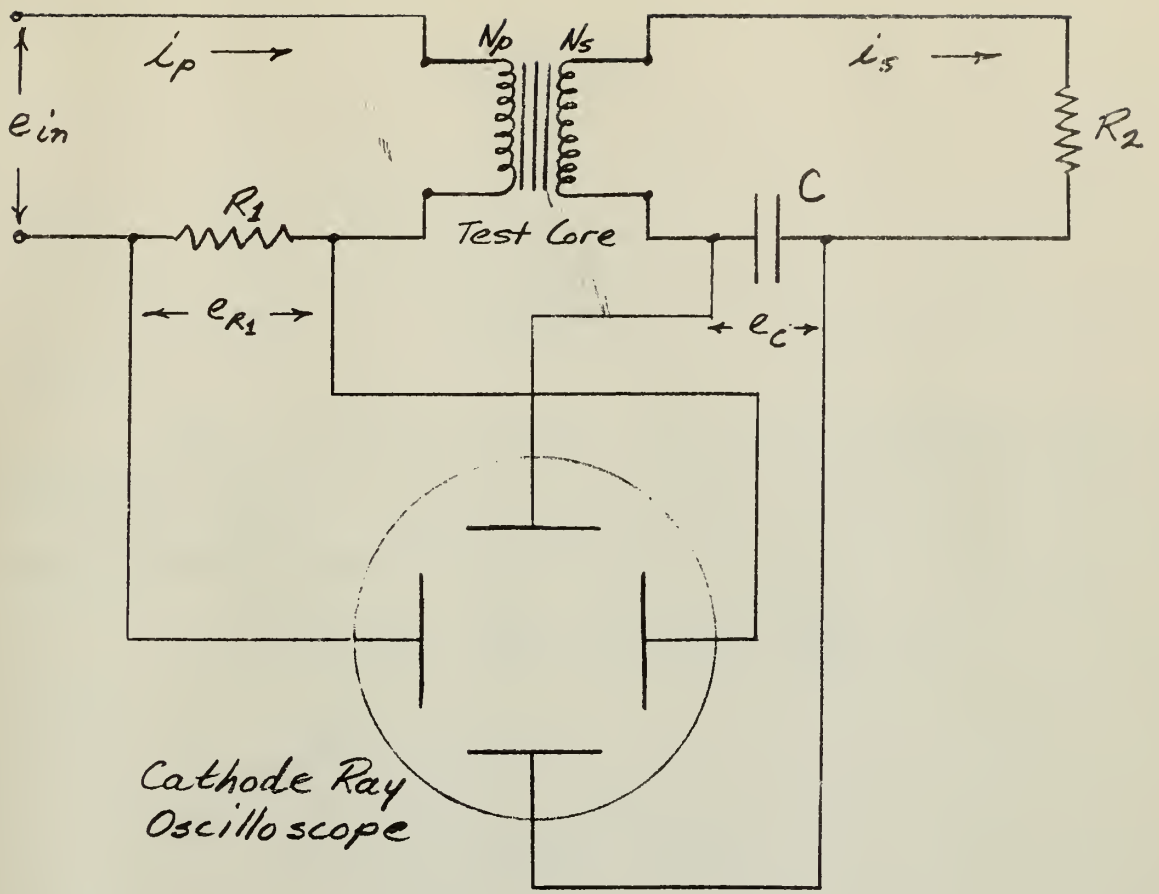

CIRCUIT FOR OBSERVATION OF MAGNETIZATION CURVES

Figure 4

TOLERANCE	MATERIAL	TITLE			
UP TO 6 / ABOVE 6 TO 24 / ABOVE 24					
DEC. DIM. ±.005 / ±.010 / ±.015	FINISH	ISSUED	USED WITH	AP'PD	DWN.
FRACT. DIM. ± 1/64 / ± 1/32 / ± 1/16					
UNLESS OTHERWISE SPECIFIED					

Federal Telecommunication Laboratories, Inc. -1

$$H = \frac{0.4\,\pi\,N_p\,i_p}{\ell_c}$$

$$D_h = k_h\,i_p\,R_1 = \frac{k_h\,R_1\,\ell_c}{0.4\,\pi\,N_p}\,H$$

18. If the time constant of the load of the secondary, R_2C, is very long compared to the period of the signal, the vertical deflection D_v, may be shown to be approximately proportional to the flux density B.

$$e_s = N_s\,\frac{d\phi}{dt} \times 10^{-8} = N_s\,A_c\,\frac{dB}{dt} \times 10^{-8}$$

$$e_s \doteq i_s\,R_2$$

$$B \doteq \frac{R_2}{N_s\,A_c \times 10^{-8}} \int i_s\,dt$$

$$e_C = \frac{1}{C}\int i_s\,dt$$

$$D_v = k_v\,e_C = \frac{k_v\,N_s\,A_c \times 10^{-8}}{R_2\,C}\cdot B$$

19. From the foregoing development the following equations may be written:

$$H = \frac{0.4\,\pi\,N_p}{\ell_c\,R_1}\,e_{R_1} \qquad (1)$$

$$B = \frac{R_2\,C \times 10^8}{N_s\,A_c}\,e_C \qquad (2)$$

20. Table I shows the experimental circuit configurations used. The core size used provided a mean-flux-path length, ℓ_c, of 4.98 cm and a core cross-sectional area, A_c, of 0.101 cm^2 for the metallic cores and an ℓ_c of 5.63 cm and an A_c of 0.099 cm^2 for the ferritic cores.

Table I

Data for Determination of Magnetization Curves

Core Material	N_p	R_1	e_{R_1} (full scale)	N_s	R_2	C	e_C (full scale)	f
			(v)			(μf)	(mv)	
Deltamax (5340)	50	66	50	100	82K	0.5	45	400 2700
Mo-Permalloy (5340)	50	470	17	100	120K	0.6	15	100 400 2700 6000
Supermalloy (5340)	75	820	19	100	120K	0.6	24	200 400 2700 6000
Ferramic H-419	150	22	150	150	120K	0.7	38	200 400 2700 600

21. Typical results obtained are shown in Figure 5. Increasing the frequency results in the expansion and unsquaring of the hysteresis loops. A reasonably close agreement between published and observed saturation flux densities is indicated by Table II.

Table II

Comparison of Observed and Calculated Saturation-Flux Densities

Core Material	Published Saturation-Flux Density	Observed Saturation-Flux Density
	(gauss)	(gauss)
Deltamax	14,000	13,000
Mo-Permalloy	6000	5350
Supermalloy	6700	5700
Ferramic H-419	2000	2400

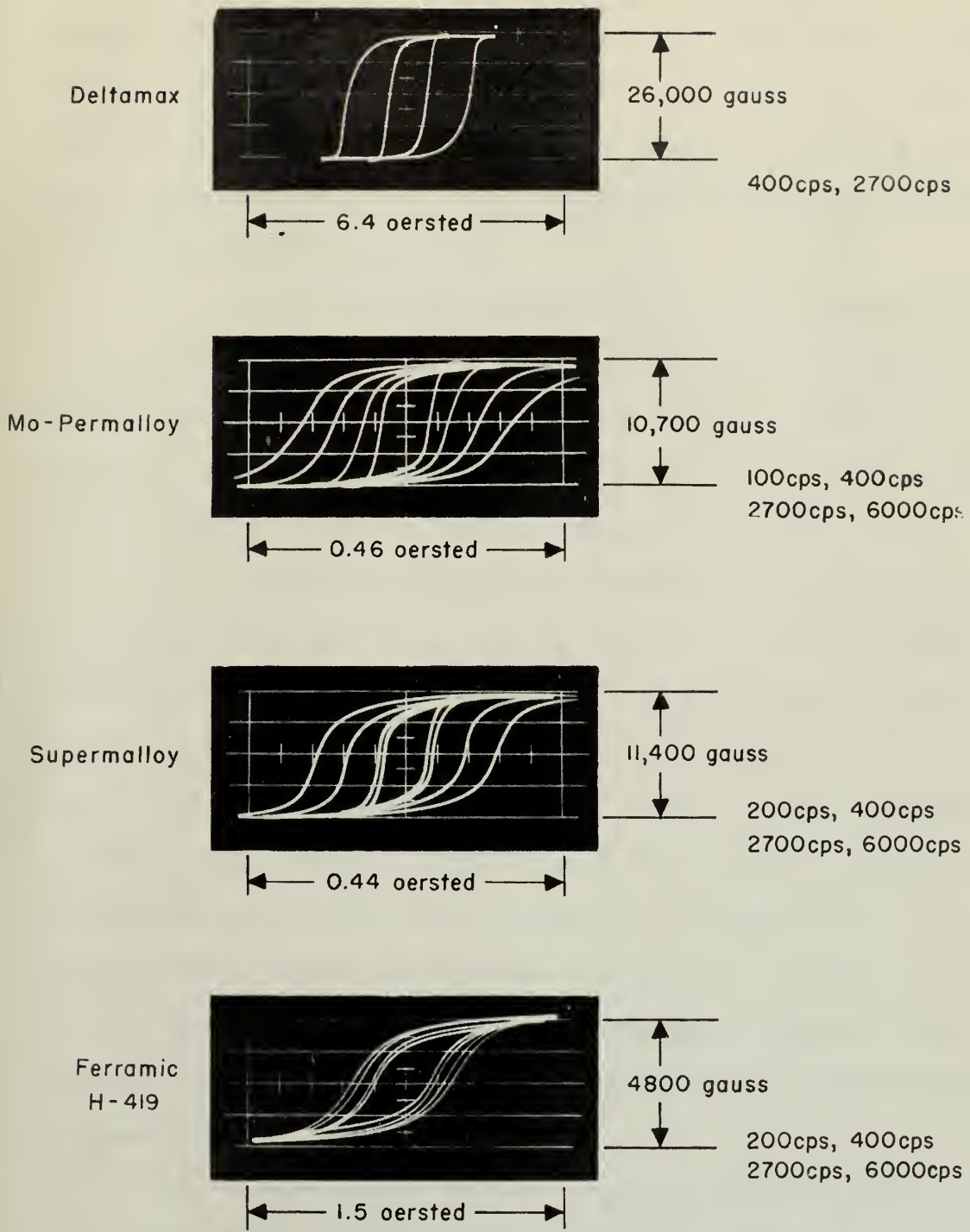

FIGURE 5
MAGNETIZATION CURVES (FREQUENCY VARIED)

22. Comparison of the published and observed 400-cps loops revealed that the width of the observed loop was nearly twice as great. This was believed due to the application of a relatively high magnetizing force drive to the cores under observation. Reduction of the drive to the point at which saturation was barely reached resulted in close agreement of published and observed loop widths.

23. The relationship between the size of the hysteresis loop and the peak magnetizing force was of sufficient importance to warrant further investigation. Figure 6 shows the variation of the loop shape of a Supermalloy core with changing peak magnetizing force. The loops are considered to be numbered in succession from the center of the pattern.

24. The relationship between the width of the hysteresis loop and the peak magnetizing force is shown graphically using both linear and semi-logarithmic plots in Figures 7 and 8. A rough generalization of the information contained in Figure 6 and the curves is that the loop width increases at a nearly constant rate until saturation is reached, at which point the rate decreases but remains fairly linear. It would be of considerable interest to extend the curves somewhat further, but the available equipment was not capable of providing greater drive without excessive distortion. Another conclusion which may be drawn is that the average permeability increases slightly until saturation is reached and then decreases linearly as the peak magnetizing force is increased.

25. It also seemed very desirable to obtain some sort of quantitative relationship between the width of the hysteresis loop and the frequency of excitation. Figure 9 shows the results of a variable frequency test of a Supermalloy core. The peak-magnetizing force at each frequency was just sufficient to produce saturation of the core.

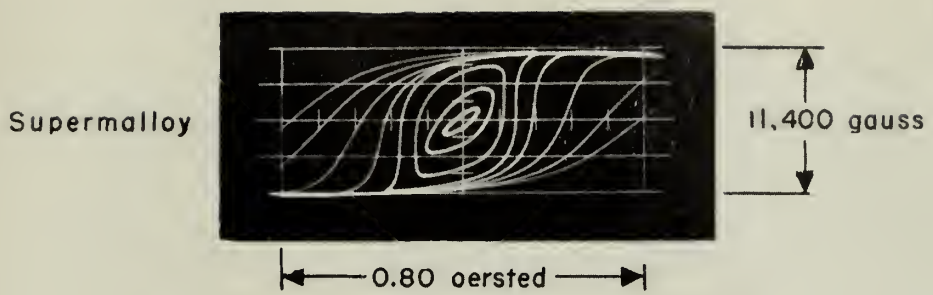

1. 0.052 oersted
2. 0.066 oersted
3. 0.085 oersted
4. 0.125 oersted
5. 0.47 oersted
6. 0.96 oersted
7. 1.49 oersted
8. 2.42 oersted

FIGURE 6
MAGNETIZATION CURVES (PEAK MAGNETIZING FORCE VARIED)

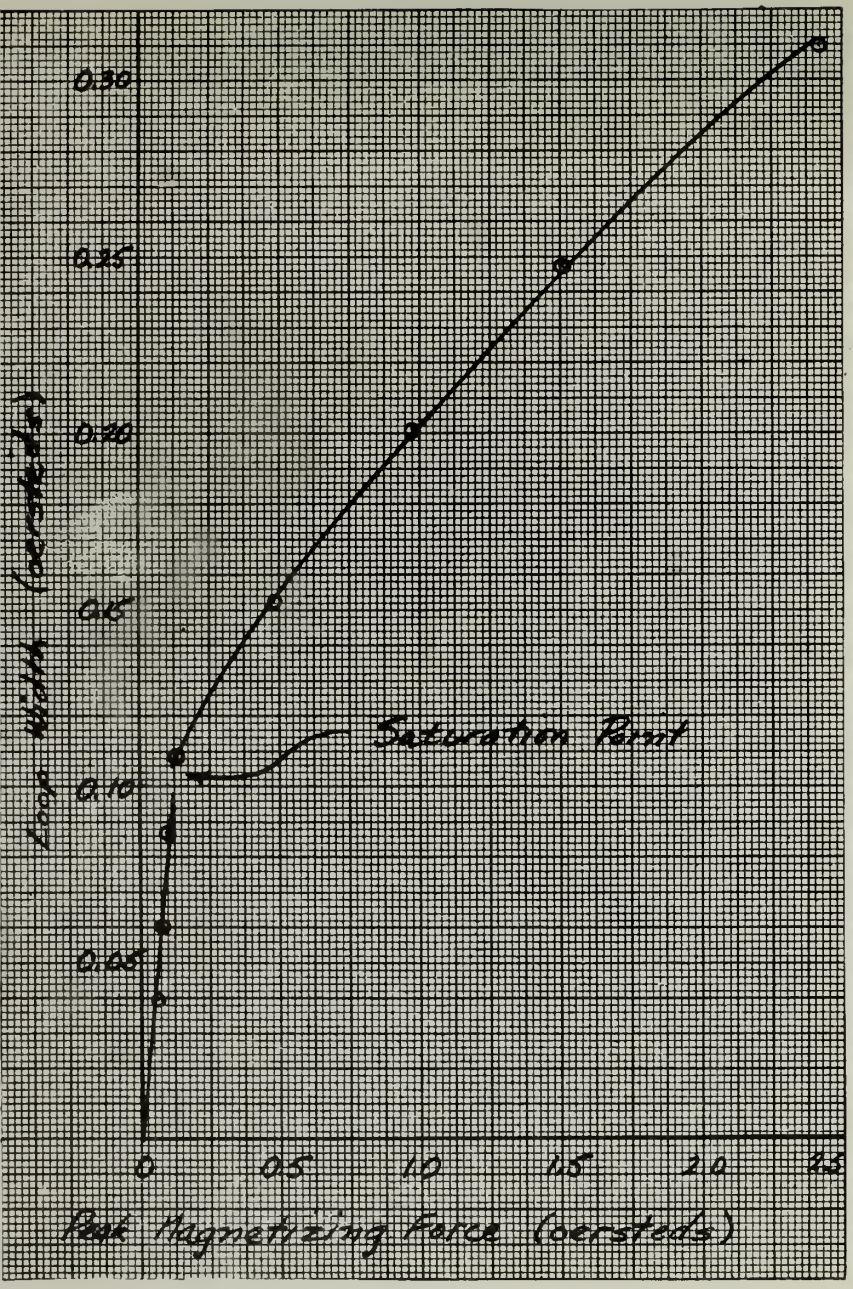

FIGURE 7
HYSTERSIS LOOP WIDTH VS. PEAK MAGNETIZING FORCE
SUPERMALLOY CORE

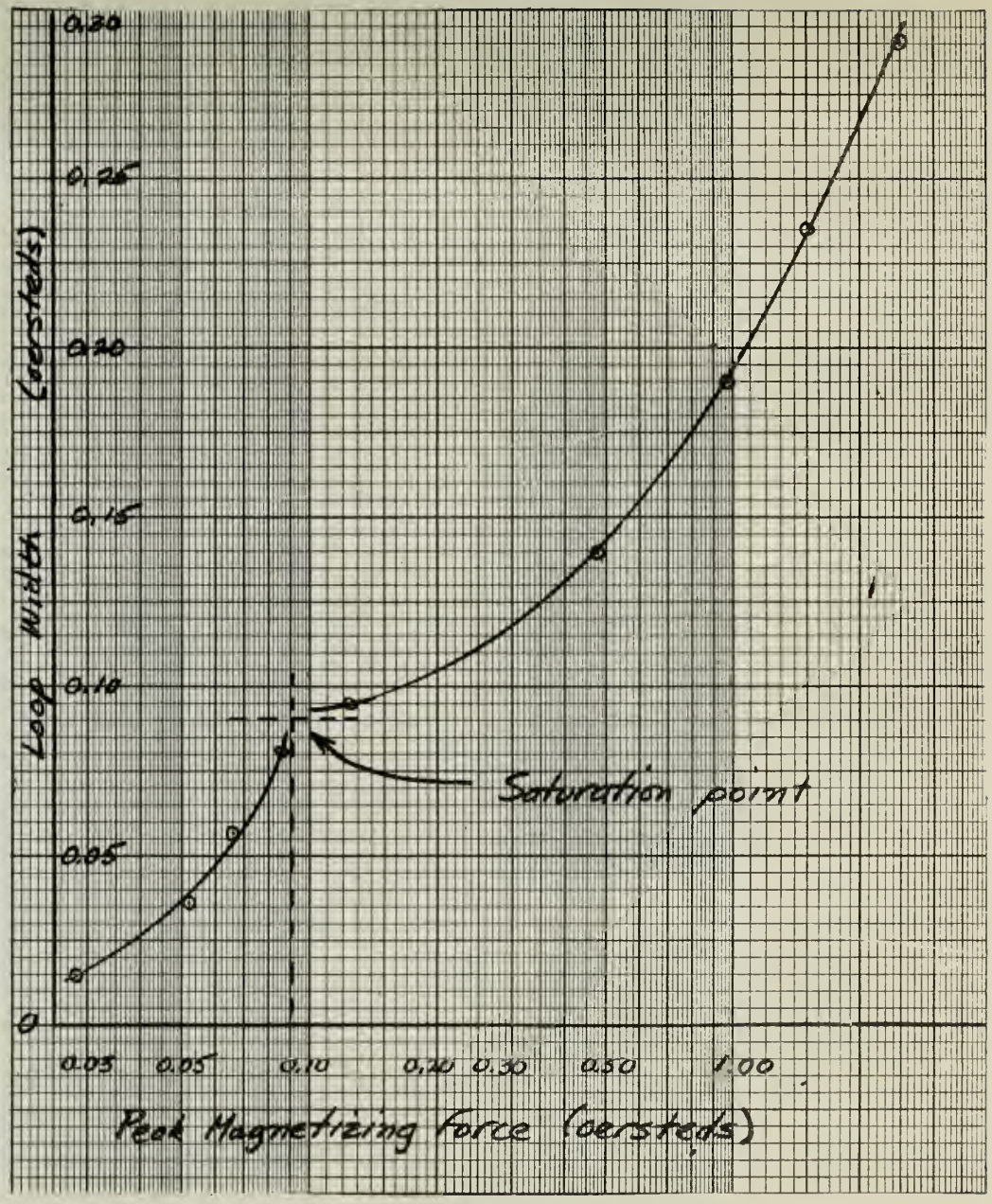

FIGURE 8
HYSTERSIS LOOP WIDTH VS. PEAK MAGNETIZING FORCE

1. 100cps
2. 400cps
3. 2700cps
4. 6000cps
5. 10,000cps
6. 20,000cps

FIGURE 9
SATURATION MAGNETIZATION CURVES (FREQUENCY VARIED)

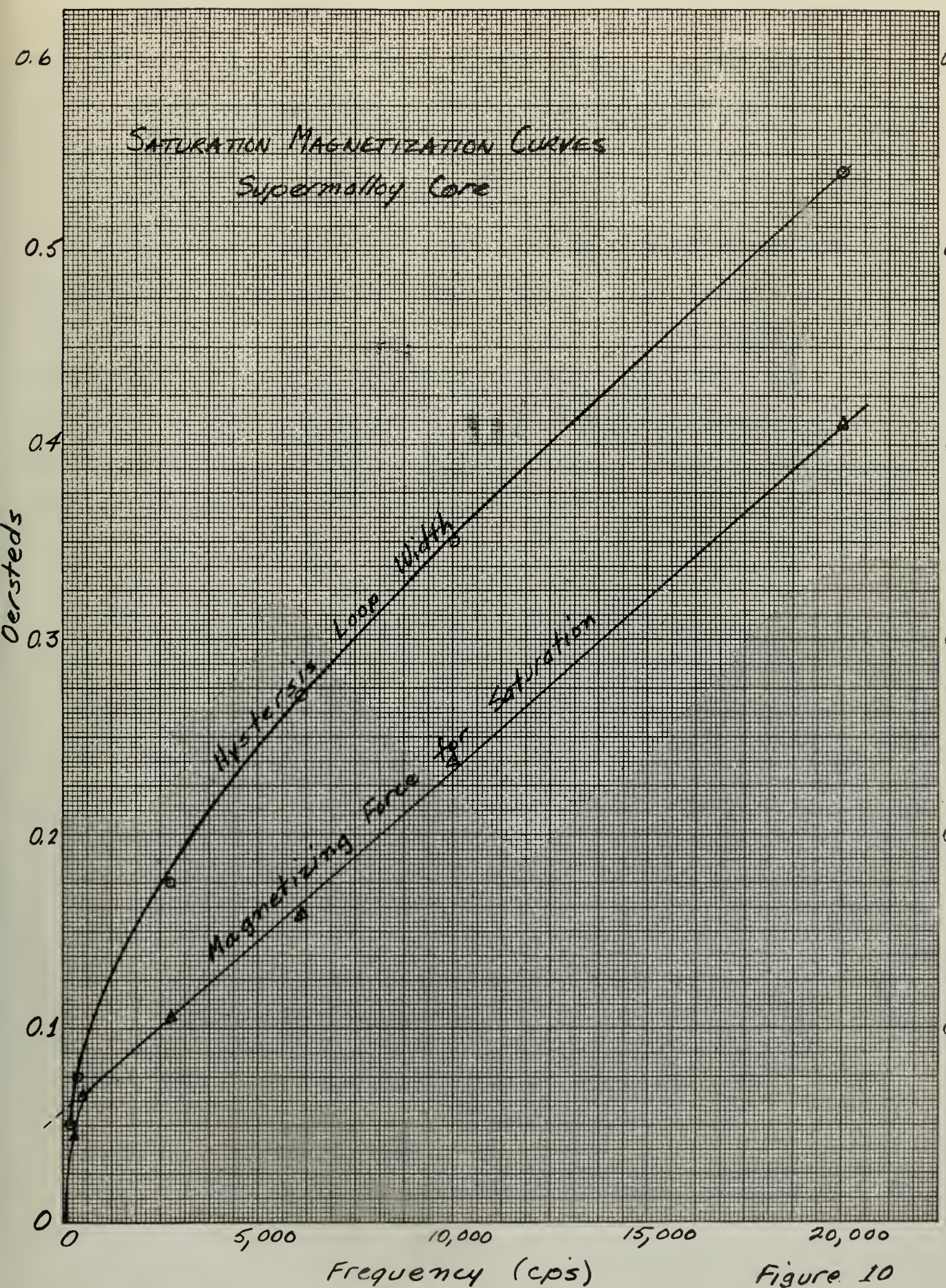
Saturation Magnetization Curves
Supermalloy Core
0.6
0.5
0.4
0.3
0.2
0.1
0
Oersteds
0
5,000
10,000
15,000
20,000
Frequency (cps)
Loop Width
Hysteresis
Saturation
Magnetizing Force

Figure 10

26. Figure 10 shows the relations of hysteresis loop width and peak magnetizing force required for saturation versus excitation frequency. The latter curve is of particular interest and may be represented above 500 cps by the following empirical relation:

$$H_s = 0.04 + 2 \times 10^{-5} f \quad \text{oersteds} \qquad (3)$$

27. Referring back to Paragraphs 23 and 24, it may be seen that another and perhaps more important relationship may be derived from the available information. This is the relation between peak magnetizing force and the time width of the hysteresis loop. Figure 11 is a graphic plot for a Supermalloy core excited at 2700 cps. As might be inferred from the previous curves, the time width of the hysteresis loop is only slightly dependent on the peak magnetizing force when this force is much greater than that required to achieve saturation.

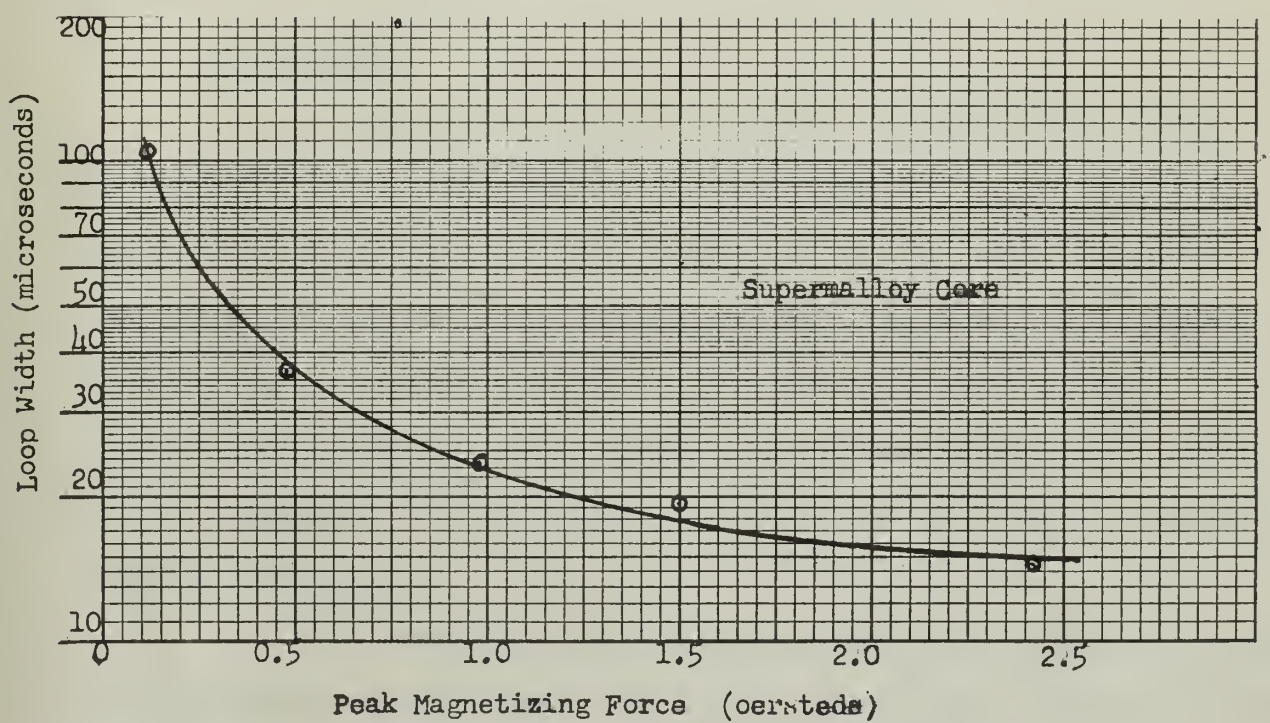

Figure 11

Loop Width (Time) vs. Peak Magnetizing Force

28. One of the cores, which are encased in nylon covers, was opened and a section of tape removed for study of the effects of physical deformation of the tape by compression, stretching, bending, twisting, etc. The tests were conducted with the tape used as the secondary core section of a magnetic circuit. No attempt was made to obtain quantitative results, but the acute susceptibility of the tape to deterioration of its magnetic properties by physical distortion was clearly demonstrated.

29. The available engineering data on the core materials indicated that temperature affects the magnetic properties of the materials, but in a relatively minor degree. For this reason and because of time limitations, no research was conducted along this line. By the same token, evaluation of changes of core properties due to aging and of variations in core properties in a sample of similar cores could not be accomplished.

C. Conclusions

30. It is apparent from the preceding paragraphs that, due to the limitations of time primarily and of equipment to a lesser extent, the research portion of the project was cursory and fairly limited in scope. Nevertheless, a good foundation in understanding the behavior of magnetic materials was gained, particularly in the areas of specific interest concerning the problems at hand. Several general conclusions may be drawn from the foregoing investigation, the most important of which are considered to be the following:

1. Increasing the frequency of excitation widens and reduces the squareness of the hysteresis loop of the core material. Above 500 cps the relation between loop width and frequency is nearly linear.

2. Increasing the peak magnetizing force widens and reduces the squareness of the hysteresis loop. The time width of the loop is reduced by increasing the peak force, but the reduction is only minor when the magnetizing force has become a few times that required for saturation.

3. Any form of physical deformation of the core material seriously affects its magnetic properties. The effects are roughly proportional to the degree of the deformation. Provided the stress applied to achieve deformation does not result in exceeding the elastic limit of the material, removal of the stress returns the material to its original magnetic state. It should be noted that the magnetic tape is extremely susceptible to permanent strain due to bending or twisitng.

III. MAGNETIC PULSE FORMERS

A. Peaking Transformer

31. The simplest type of magnetic pulse former is shown in Figure 12. The output pulses are generated as the core is driven from saturation of one polarity to the other. As a result of the lag of the current in the input circuit, whose impedance is primarily inductive reactance, the output pulses lag the excursions of the input voltage through zero by nearly 90 degrees.

32. In order to achieve a rise time of one microsecond in the output pulse, Δt has a maximum value of approximately two microseconds or slightly less than two degrees expressed angularly. Saturation reversal must occur during a current amplitude change, ΔI, of $I_{max} \sin 2^{\circ}$. The core thus must be saturated when the current has reached $0.017\ I_{max}$.

33. Selection of the core material must be based on two parameters: (1) the incremental permeability in the unsaturated region, which

PEAKING TRANSFORMER

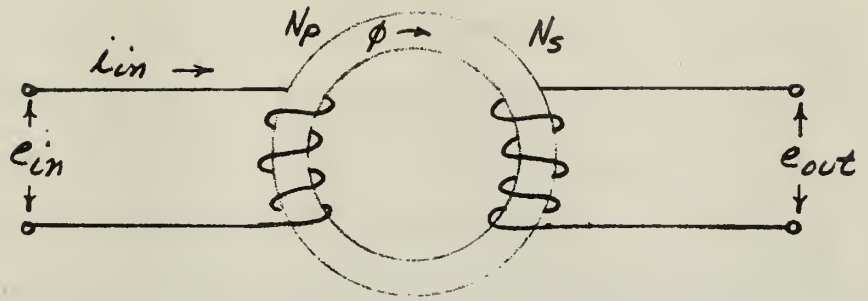

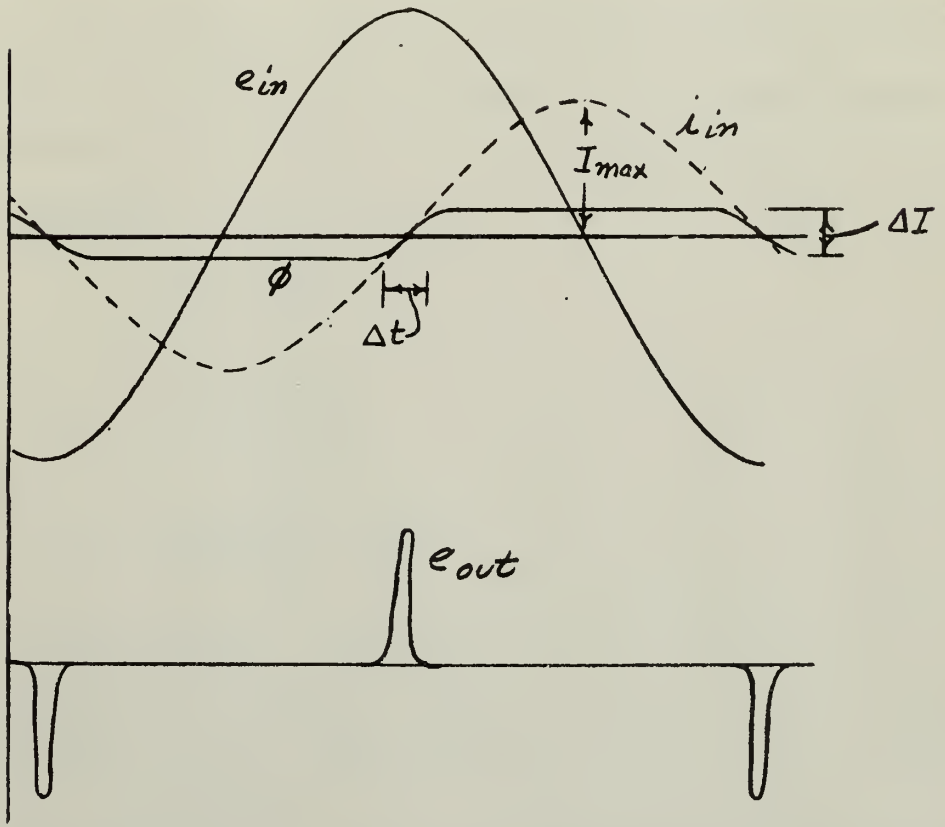

Figure 12

TOLERANCE				MATERIAL	TITLE			
	UP TO 6	ABOVE 6 TO 24	ABOVE 24					
DEC. DIM.	±.005	±.010	±.015					
FRACT. DIM.	± 1/64	± 1/32	± 1/16	FINISH	ISSUED	USED WITH	AP'PD	DWN.
UNLESS OTHERWISE SPECIFIED								

Federal Telecommunication Laboratories, Inc. -1

will determine the effective inductance of the coil and hence the amount of current which will flow for a given magnitude of source voltage; and (2) the magnetizing force required to saturate the core. Since the time required for the reversal of saturation flux polarity should be as small as possible, it is apparent that both of the above factors should be minimized. Unfortunately, a brief survey of available core materials indicates that a low incremental permeability is characteristic of materials which are difficult to saturate while those materials most readily saturated possess relatively high incremental permeability.

34. The following nonrigorous development was made to relate these two critical factors to the performance of the proposed circuit. Volt-amperes required for saturation is the performance criterion. (The subscript s denotes saturation values.)

$$L = \frac{4\pi \times 10^{-9} A_c}{\ell_c} N_p^2 \mu$$

$$H_s = \frac{0.4\pi N_p I_s}{\ell_c}$$

$$I_s = \frac{\ell_c}{0.4\pi N_p} H_s$$

$$V_s = I_s X_L = 2\pi f I_s L$$

$$V_s I_s = 5 \times 10^{-8} \ell_c A_c f H_s^2 \mu \qquad (4)$$

$$= K_1 H_s^2 \mu$$

The above development assumes leakage flux and losses due to hysteresis and eddy currents to be negligible. The absence of the number of primary turns from the derived relation is of special interest.

35. A comparison of the suitability of the available materials is shown in Table III. The total volt-amperes required for the best materials,

Supermalloy and Ferramic H-419, are than 180 and 155 respectively as compared to the one volt-ampere available.

Table III

Comparison of Volt-Amperes Required for Saturation

Core Material	K_1	H_s	μ	$H_s^2\mu$	V_sI_s
Deltamax	6.80×10^{-5}	0.8	50,000	32,000	2.18
Mo-Permalloy	6.80×10^{-5}	0.2	50,000	2000	0.136
Supermalloy	6.80×10^{-5}	0.08	150,000	960	0.065
Ferramic A-34	7.52×10^{-5}	6.0	97	3500	0.234
Ferramic C-159	7.52×10^{-5}	2.5	710	4450	0.303
Ferramic H-419	7.52×10^{-5}	0.5	3300	825	0.056

36. From these results it is readily apparent that the proposed type of device using presently available cores falls far short of meeting the limiting specifications. The chief impediment is the difficulty of a achieving rapid saturation of the core. Rewriting equation (4),

$$V_sI_s = 5 \times 10^{-8} f \left[\ell_c A_c\right] \left[H_s^2 \mu\right]$$

it is seen that the first bracket contains those factors relating to core dimensions and the second those dependent on core material. Since it is unlikely that any particular improvement in core material can be achieved, reduction of core cross-sectional area and mean-flux-path length is indicated.

For instance, the core might be formed from one or two narrow loops of 1-mil Supermalloy tape as opposed to the present smallest size core, the 5340 series, composed of some 115 turns of 1/4 inch, 1-mil tape.

37. Two major difficulties deter the use of such a core as suggested above. The reduction of the pulse amplitude by a factor a one-hundredth could not likely be avoided by a reciprocal increase in the number of output turns because of the effects of distributed capacity in reducing response time. Also, with the core's high reluctance, due to its extremely small cross-sectional area, leakage inductance would assume formidable proportions.

38. The driving-point impedance seen by the voltage source will be very nonlinear in this type of device because of the wide difference of inducatance levels between the saturated and unsaturated conditions of the core. To avoid in large measure this highly undesirable condition, a choke or resistor load may be inserted in series with the reactor coil. For an optimum condition, this series impedance probably should be approximately the geometric mean of the saturated and unsaturated impedance of the reactor coil.

B. Peaking Transformer with Shunt

39. Another method of achieving the above result is shown in Figure 13. The operation of this device in producing pulses is basically the same as previously described, with the small cross-sectional area of the output leg of the core permitting a very rapid reversal of saturation-flux polarity. The shunt leg provides a nonsaturating flux path to present an essentially constant load to the driving source. The air gap prevents shunting of all the primary flux and the accompanying reduction of the output voltage to zero.

40. This device was adapted to a more convenient configuration as indicated by Figure 14. A standard Hipersil (Westinghouse) core, represented

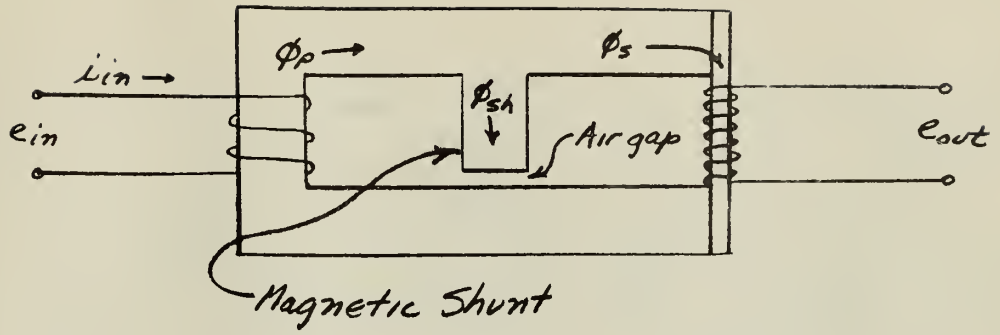

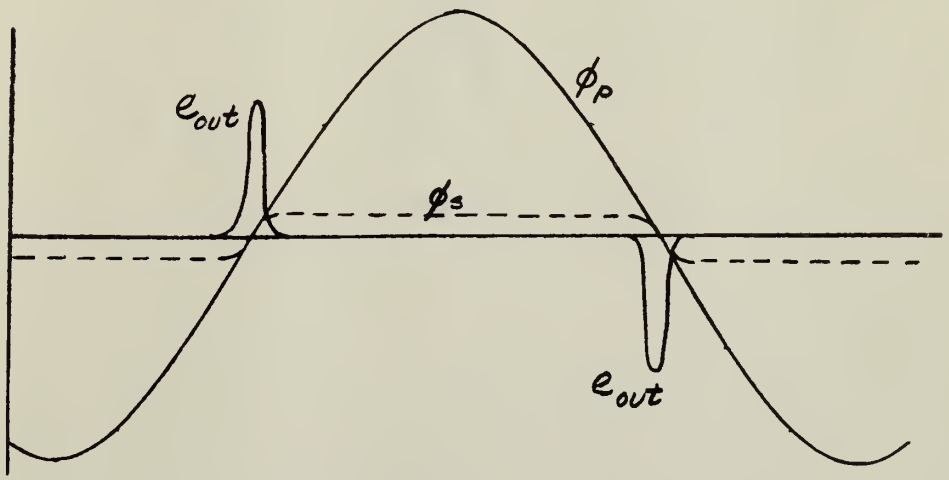

PEAKING TRANSFORMER WITH SHUNT

Figure 13

TOLERANCE	MATERIAL	TITLE			
UP TO 6 / ABOVE 6 TO 24 / ABOVE 24					
DEC. DIM. ±.005 / ±.010 / ±.015					
FRACT. DIM. ± 1/64 / ± 1/32 / ± 1/16	FINISH	ISSUED	USED WITH	AP'PD	DWN.
UNLESS OTHERWISE SPECIFIED					

Federal Telecommunication Laboratories, Inc. -1

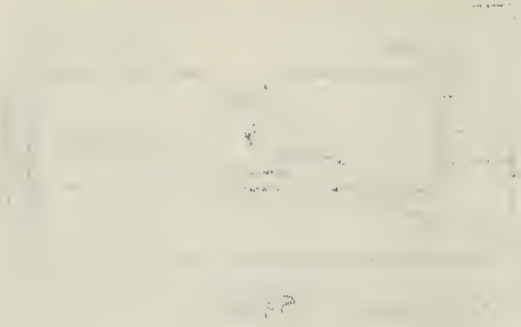

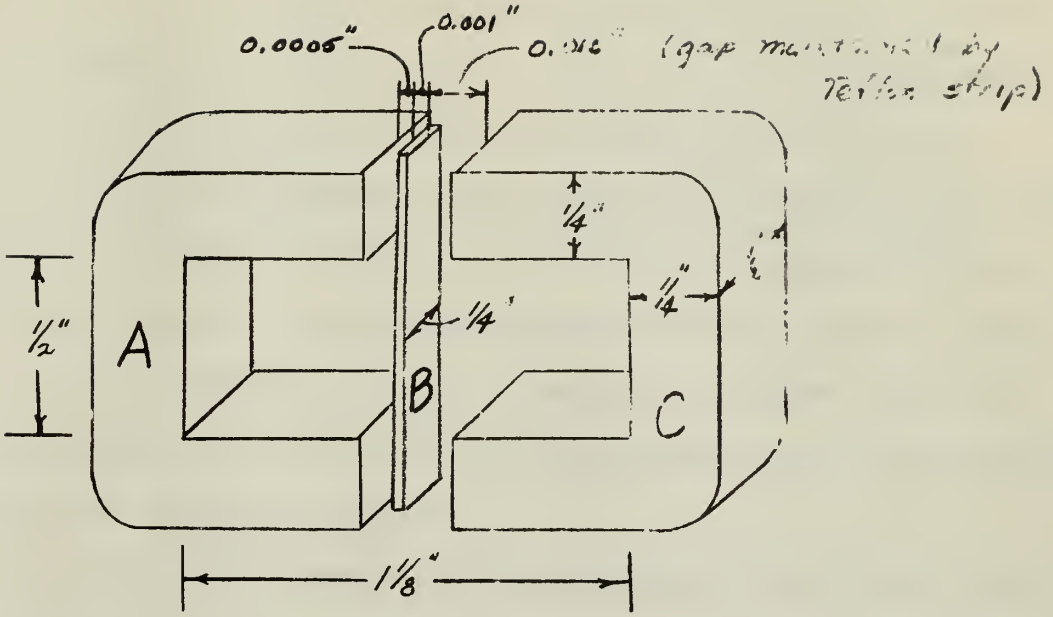

CORE CONFIGURATION OF PEAKING TRANSFORMER

Figure 14

TOLERANCE				MATERIAL	TITLE			
	UP TO 6	ABOVE 6 TO 24	ABOVE 24					
DEC. DIM.	±.005	±.010	±.015					
FRACT. DIM.	± 1/64	± 1/32	± 1/16	FINISH	ISSUED	UNLESS WITH	AP'PD	DWN.
UNLESS OTHERWISE SPECIFIED								
Federal Telecommunication Laboratories, Inc.								-1

by the sections labeled A and C, was used, with the primary winding on A. The core is formed of 5-mil silicon-steel laminations which are grain-oriented. The output winding was on core B, a section of 1/4-inch, 1-mil Supermalloy tape, and the spacer which maintained the gap was a 10-mil strip of Teflon.

41. Using the experimental data previously described, preliminary calculations (see Appendix A) indicated that a driving voltage of 70 volts rms, a 1000-turn primary, and a 400-turn secondary should produce an output pulse of 13.2 volts amplitude and 5.6 microseconds rise time. This is in fairly close agreement with the 12-volt, 8-microsecond rise-time pulse which resulted when the circuit was tested.

42. The lack of agreement between calculated and observed pulses may be attributed to the following basic causes: (1) delays introduced by electrical circuit parameters; (2) inherent time lag in the magnetic response of the core material; (3) deterioration of magnetic properties of the core materials due to cutting and handling of the tape; and (4) errors introduced during interpolation of experimental and published data.

43. Typical output pulses and a photograph of the actual pulse former are shown in Figure 15. The lack of symmetry of the pulse is due to the characteristic shape of the Supermalloy hysteresis loop. Table IV shows the results of the most significant tests made, using varying air gaps and different secondary core sizes and materials.

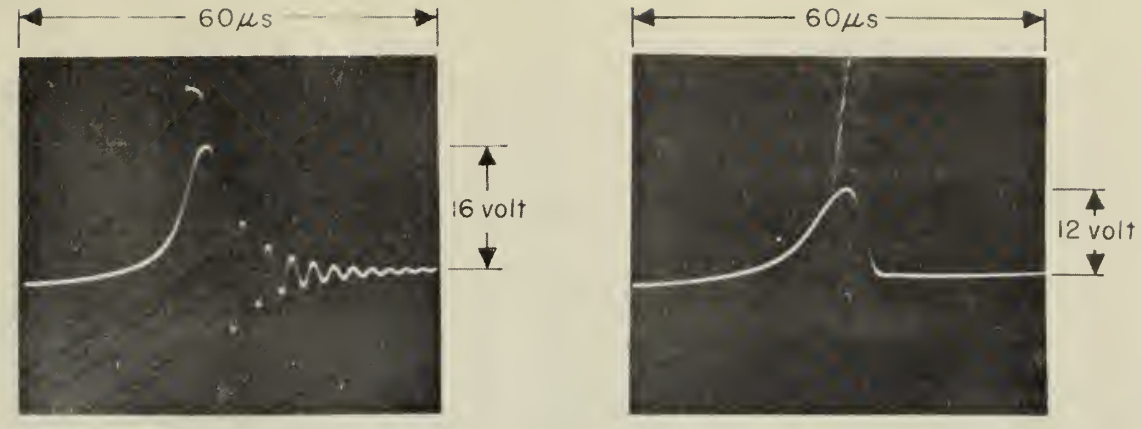

Open circuit termination

3000 ohm termination

OUTPUT PULSES

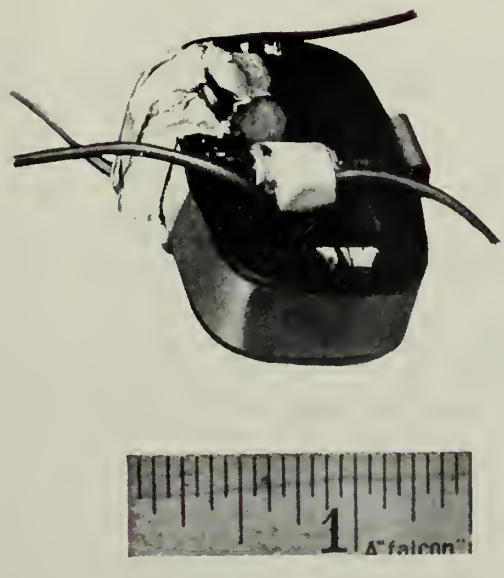

PEAKING TRANSFORMER WITH SHUNT

FIGURE 15

Table IV

Peaking Transformer Test Results

	Core Material	Core Width	Core Thickness	Gap Size	Primary Voltage	Primary Current	Pulse Rise Time	Pulse Fall Time	Pulse Height
		(in.)	(mils)	(mils)	(v)	(ma)	(μsec)	(μsec)	(v)
1	Supermalloy	1/4	1	20	70	11.6	8	2	12
2	Supermalloy (crumpled)	1/4	1	20	70	11.6	12	3	4
3	Supermalloy	1/32	1	20	70	11.6	3 (much 2700 cps)	2	3.5
4	Supermalloy	1/16	1	20	70	11.6	5	1	2.5
5	Supermalloy	1/16	1	40	50	16.7	5	1	2.5
6	Supermalloy	1/4	1	20	70	11.6	10	2	10
7	Carpenter "49"	1/8	6	20	70	11.6	—	—	0
8	Supermalloy	1/4	1	20	70	11.6	8	1.5	10
9	Supermalloy	1/4	1	40	50	16.7	6	1	10
10	Supermalloy	1/4	1	60	40	20	5	1	8
11	Deltamax	1/8	1	20	70	11.6	6	2	10
12	Deltamax	1/8	1	40	50	16.7	5	2	10
13	Deltamax	1/24	1	40	50	16.7	4	2	3

44. Because of its relatively square hysteresis loop, a section of 1/8-inch, 1-mil Deltamax tape was tested for use as the secondary core. The output pulses were comparable to those of the Supermalloy core, and, as predictable from the shape of the Deltamax loop, the output pulse was more nearly symmetrical.

45. Except for its nearly constant input impedance and ease of construction (no toroidal cores to wind), this device offers no real improvement over the simple peaking transformer discussed initially. As explained in Paragraph 37, leakage inductance and low pulse amplitude discourage reduction of the secondary core size. However, the relatively steep trailing edge of the output pulse when Supermalloy tape was used suggested a different line of attack.

C. Regenerative Pulse Former

46. An RC differentiating circuit was connected across the output of the peaking transformer of Figure 14. The resultant wave shape was similar to the previous observations, but close examination showed the fall time to be slightly less and the overshoot to be slightly greater. This phenomenon is not possible from the standpoint of a purely differentiating action and can only be explained as the indication of some form of regeneration.

47. Since the effects of leakage inductance, which are relatively large due to the small cross-sectional area of the secondary core, tend to mask the triggering action, the circuit shown in Figure 16(a) was tried. The saturable core reactor, L_2, was a standard 5340 Supermalloy core with a winding of 225 turns. The L_1C_1 network established an input resonance at 2700 cps and thus provided a nearly constant-current drive of L_2.

48. Excellent results were obtained from this circuit, whose operation may be explained by reference to Figure 16(b). When saturated, L_2 may be

(a)

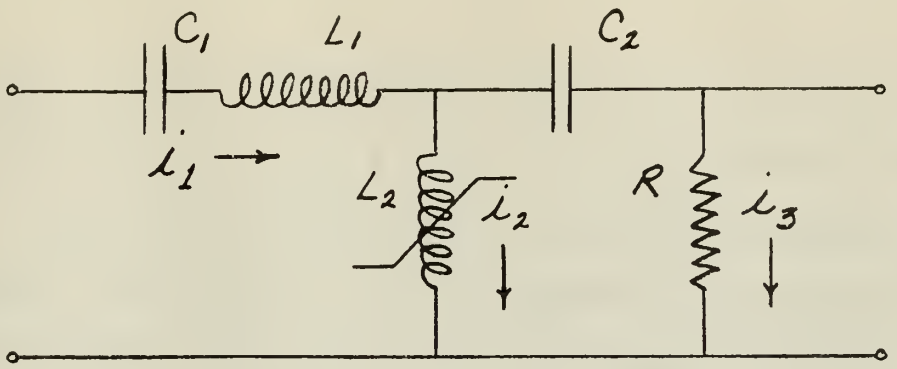

(b)

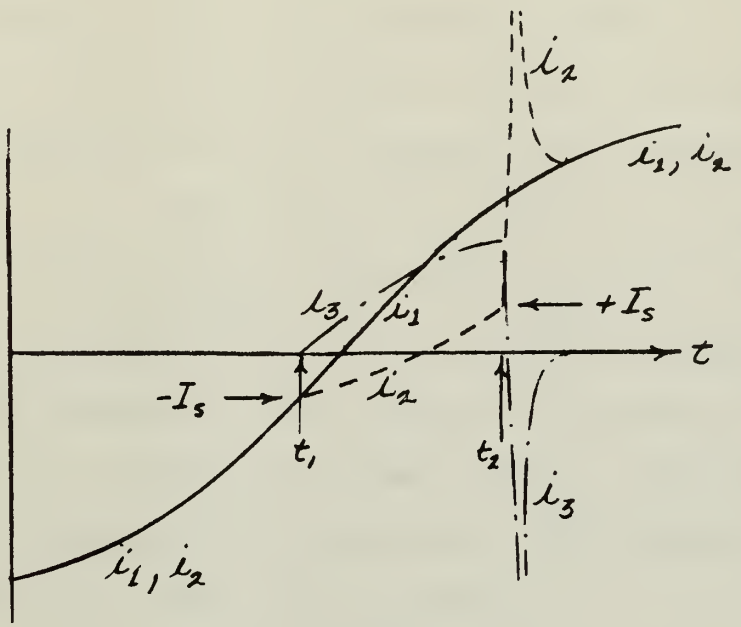

REGENERATIVE PULSE FORMER

Figure 16

TOLERANCE	MATERIAL	TITLE			
UP TO 6 / ABOVE 6 TO 24 / ABOVE 24					
DEC. DIM. ±.005 / ±.010 / ±.015	FINISH	ISSUED	USED WITH	AP'PD	DWN.
FRACT. DIM. ± 1/64 / ± 1/32 / ± 1/16					
UNLESS OTHERWISE SPECIFIED					

Federal Telecommunication Laboratories, Inc. -1

considered a virtual short circuit. Thus, prior to t_1, all the input current, i_1, flows through L_2 ($i_1 = i_2$, $i_3 = 0$), and the voltage across C_2 is zero.

49. At t_1, the core becomes unsaturated and presents a high impedance to the flow of i_1, which is maintained sinusoidal by L_1C_1. Capacitor C_2 then charges slowly until t_2, when i_2 is again sufficiently large to commence driving the core into the saturation region.

50. The resulting decrease of voltage across L_2 due to its reducing impedance permits C_2 to discharge through L_2 and produce the output voltage pulse, $i_3 R$. The discharge of C_2 through L_2 is regenerative in nature. If R and L_2 are sufficiently small, C_2 is able to supply a high current nearly instantaneously. Thus as the effective inductance of the saturable core reduces due to its approach to saturation, the discharge current from C_2 is permitted to increase. This in turn hastens the saturation of L_2, and the resulting cumulative action results in an output pulse with a steep leading edge and high amplitude.

51. Using a signal generator with a low output impedance, the test circuits shown in Figure 17 were set up. The transformer was required for impedance matching. Table V shows the results of the most significant tests.

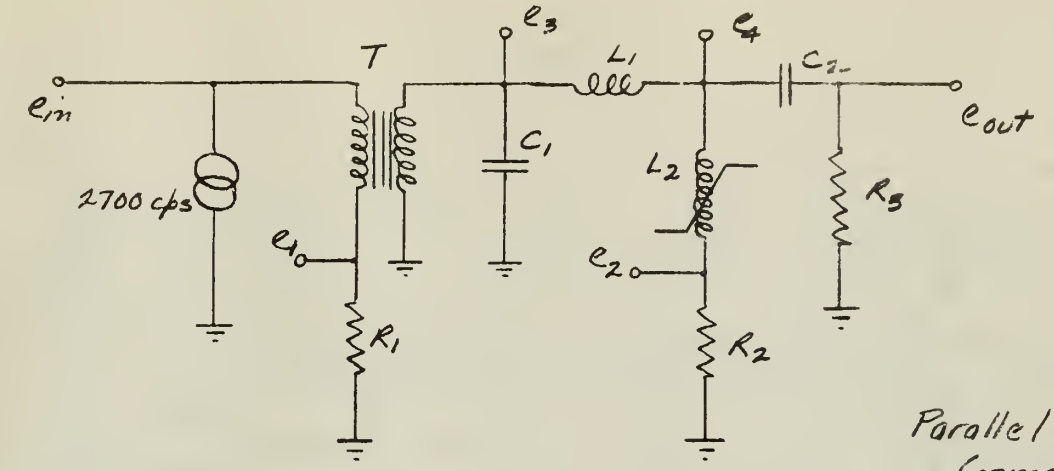

Parallel Connection

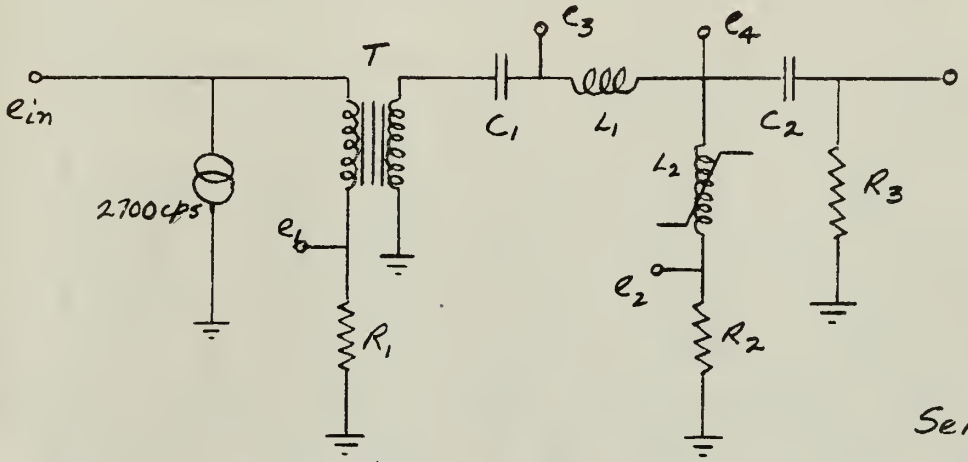

Series Connection

TEST CIRCUITS FOR TABLE V

Figure 17

TOLERANCE				MATERIAL	TITLE			
	UP TO 6	ABOVE 6 TO 24	ABOVE 24					
DEC. DIM.	±.005	±.010	±.015					
FRACT. DIM.	± 1/64	± 1/32	± 1/16	FINISH	ISSUED	USED WITH	AP'PD	DWN.
UNLESS OTHERWISE SPECIFIED								

Federal Telecommunication Laboratories, Inc. -1

Table V

Regenerative-Pulse-Former Tests (See Figure 17)

L_2	5340-S1 225 turns	5340-S1 150	5340-S1 75	H-419 450	H-419 300	5340-P1 150	5340-P1 100	5340-S1 225
Connection	Parallel	Parallel	Parallel	Parallel	Parallel	Parallel	Parallel	Series
Generator	650 A Osc. BA-4A Amp	→	→	→	→	→	→	→
Transformer	6.3-0 / 435-435	→	→	→	→	→	→	6.3-0 / 115-0
e_{in}	1.42 v	1.37	1.45	2.83	2.97	1.27	1.31	1.42
e_1	0.39 v	0.35	0.34	1.17	0.85	0.39	0.39	0.25
R_1	1 Ω	→	→	→	→	→	→	→
i_1	0.39 a	0.35	0.34	1.17	0.85	0.39	0.39	0.35
$V\text{-}A_{in}$	0.54	0.48	0.49	3.30	2.53	0.49	0.51	0.36
L_1	430 mh	450	480	440	460	450	475	420
C_1	.007 μf	→	→	→	→	→	→	→
e_3	113 v	120	132	290	300	141	145	113
e_4 (peak)	150 v	86	40	170	126	100	57	140
e_4 (rms)	0.16 v	0.168	0.178	0.39	0.39	0.152	0.155	0.13
e_2 (peak)	2.1 v	0.75	0.17	1.10	0.55	0.38	0.31	2.2
R_2	10 Ω	→	→	→	→	→	→	→
i_2 (rms)	16 ma	16.8	17.8	39.0	39.0	1.52	1.55	13.0
i_2 (peak)	210 ma	75	17	110	55	38	31	220
C_2	.001 μf	→	→	→	→	→	→	→
R_3	500 Ω	→	→	→	→	→	→	→
e_{out} (peak)	100 v	59	7	100	86	46	9	100
Rise Time	0.7 μsec	2.0	7.0	5.0	5.0	2.0	8.0	0.7

52. The tests indicated the superiority of Supermalloy cores over the other materials, but the performance of the Mo-Permalloy cores was nearly as good. Because of the similarity in performance of the parallel and series input connections, only the most favorable series test is included in the table.

53. The results were obviously extremely encouraging and invited a reassessment of the original specifications. Direct drive from an indicating-instrument resolver would be particularly desirable. A typical synchro-resolver would have an internal impedance of 2500 ohms at 2700 cps and be capable of delivering about 0.2 volt-amperes.

54. For apparent reasons it would be desirable to substitute a resistance load for the L_1C_1 tuned circuit. Table VI shows the results of several tests made using a resistance input, R_L. The most significant portion of the table is the phase-shift section, which indicates that the device is inherently sensitive to amplitude changes in the driving voltage. The observed phase shift is greater than can be tolerated since, in order to maintain a pulse-position accuracy of $\pm$ 1/2 microsecond, it would be necessary to regulate the driving voltage to within one per cent. The resistance input circuit was therefore abandoned.

Table VI

Regenerative-Pulse-Former Test (Resistance Input)

Test		1	2	3	4	5	6	7	8
Core		5340-P1	5340-P1	5340-S1	5340-S1	5340-P1	5340-P1	4168-S1	5340-P1
Turns		150	100	225	150	250	350	500	300
R_L		4000 Ω	4000	6500	6500	4000	4000	9000	4000
C_2		0.01 μf	0.01	0.01	0.01	0.01	0.01	0.01	0.01
R		270	270	270	270	270	270	270	270
e_{in}		40	40	40	40	40	40	60	40
Pulse Amplitude		25 v	12.5	25	22.5	32	30	30	28
Pulse Rise Time		1 μsec	2	1.5	2	1	1.5	2	1
Volt-Amperes		0.4	0.4	0.24	0.24	0.4	0.4	0.4	0.4
Phase Shift with Variations of e_{in}	+10%	——	-5 μsec	-8	-7	-8	-15	-10	——
	-10%	——	+5 μsec	+8	+7	+10	+20	+10	——

55. To simulate actual operating conditions a Kearfott Synchro-Resolver, Type R-235-1-A, was used as the driving source in obtaining the detailed test data which is contained in Table VII. This resolver has an output impedance of 760 + j2710 ohms or 2870 $\varepsilon^{j15.6^\circ}$ ohms at 2700 cps. Figure 18 shows the circuit configuration used during the tests.

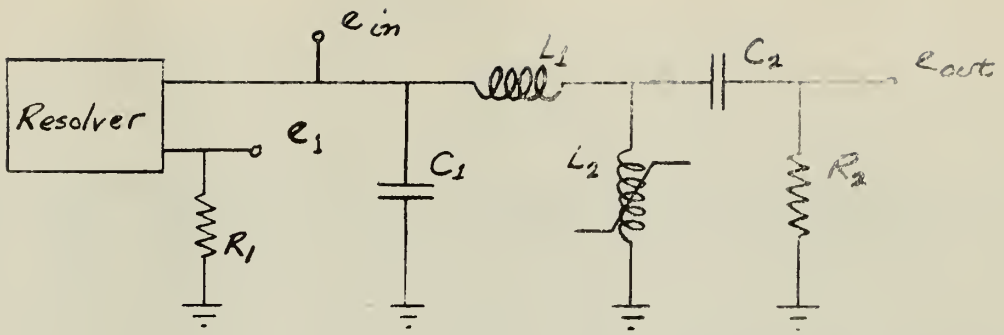

Parallel Connection

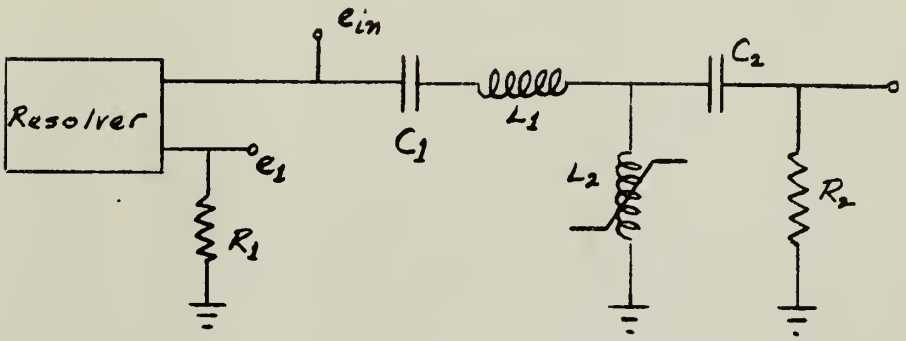

Series Connection

TEST CIRCUITS FOR TABLE VII

Figure 18

TOLERANCE	MATERIAL	TITLE			
UP TO 6 / ABOVE 6 TO 24 / ABOVE 24					
DEC. DIM. ±.005 / ±.010 / ±.015					
FRACT. DIM. ± 1/64 / ± 1/32 / ± 1/16	FINISH	ISSUED	USED WITH	AP'PD	DWN.
UNLESS OTHERWISE SPECIFIED					

Federal Telecommunication Laboratories, Inc. -1

Table VII

Regenerative-Pulse-Former Tests (See Figure 18)

Test	1	2	3	4	5	6	7	8	9	10
Core	5340-S1	5340-S1	5340-S1	5340-S1	4168-S1	4168-S1	5340-P1	5340-S1	5340-P1	5340-P1
Turns	225	150	225	150	500	1000	900	225	600	900
Connection	Par.	Par.	Par.	Par.	Par.	Par.	Par.	Par.	Par.	Ser.
e_1	0.35 v	0.28	0.45	0.35	0.43	0.50	0.40	0.30	0.23	1.50
R_1	220 Ω	220	220	220	220	220	220	220	220	220
C_1	.007 μf	.007	.007	.007	.005	.002	.007	.007	.007	.007
L_1	430 mh	480	390	510	140	110	400	360	460	380
C_2	.004 μf	.004	.003	.004	.004	.003	.002	.002	.002	.003
R_2	470 Ω	470	470	470	470	470	470	470	470	470
e_{in}	40 v	40	60	60	60	60	60	60	60	14
Pulse Amplitude	37.5 v	25	60	30	37.5	55	47	64	34	47
Pulse Rise Time	1 μsec	4	3/4	1-1/2	1-1/2	1-1/4	1	3/4	2	1
Power	63 mw	51	120	96	117	136	82	109	63	95
Phase Shift with Variations of e_{in} +10%	-3.5 μsec	-3.5	-3.0	-3.5	-5.0	-4.0	-1.75	-2.5	-2	-10
Phase Shift with Variations of e_{in} -10%	+3.5 μsec	+4.0	+3.5	+4.0	+6.0	+5.0	+2.25	+2.5	+2.5	+12
Remarks						100 mh in series with input	Core area 1/4 normal		Core area 1/4 normal	Core area 1/4 normal

56. Study of the table indicates that the standard Supermalloy core, 5340-S1, as driven in Test 8 will provide satisfactory results. This is not considered to be an optimum performance condition however. Test 7 shows the promising effects of reducing the core size, accomplished in this case by unwinding tape from a standard Mo-Permalloy core. The indications are that a Supermalloy core of smaller cross-sectional area and more turns will give best results. The series-resonant input connection is shown by Test 10 to be completely unsatisfactory because of excessive phase shift with variations of driving voltage.

57. To provide a complete picture of the generation of pulses, voltage wave forms at the critical points of the circuit shown in Figure 19 were photographed. Resistors R_1 and R_3 were required only for observation of current wave forms. Inductor L_2 was a 5340 Supermalloy core with a winding of 225 turns. Parameters L_1, C_2, R_2, and the voltage at point A had the values indicated in the circuit diagram except as noted in Figures 20 and 21, where the wave forms are displayed.

58. The basic circuit as shown in Figure 19 is considered nearly optimum for the core used. Increasing L_1, with appropriate decrease of C_1 to maintain tuning, results in a higher Q circuit and an inadequate phase stability; reducing L_1 causes an increase of pulse rise time and a decrease of pulse amplitude. Increasing or decreasing the number of turns on L_2 has in general the same effect as changes of L_1. Figures 21(d) and 21(e) indicate the results of changing C_2 and R_2. If the product R_2C_2 is kept constant, little change of pulse shape occurs. However, the combination as indicated results in the lowest input power to the circuit. Fortunately none of these values is at all critical. Any component values within the reasonable vicinity of those listed may be used.

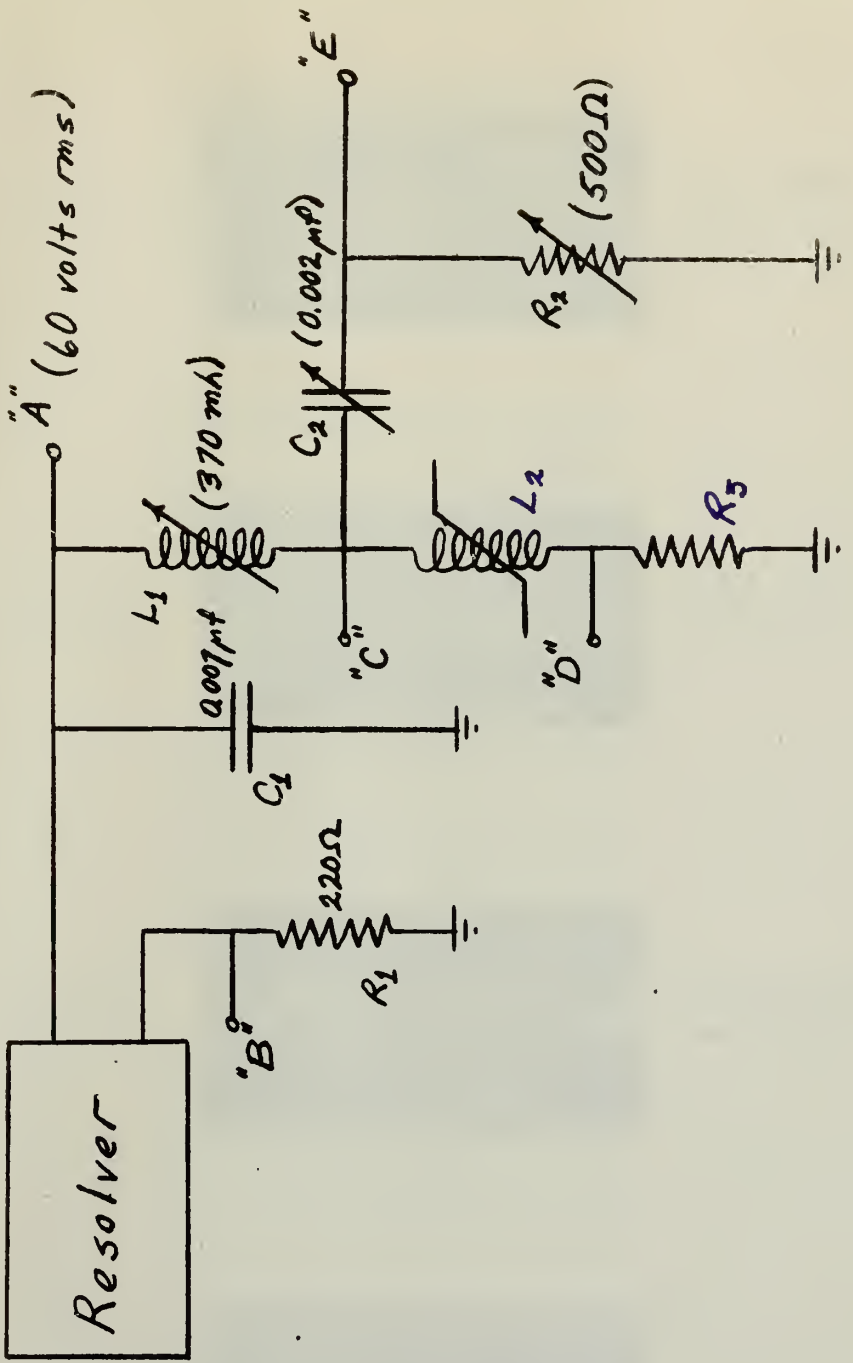

REGENERATIVE PULSE FORMER

Figure 19

TOLERANCE	MATERIAL	TITLE			
UP TO 6 / ABOVE 6 TO 24 / ABOVE 24					
DEC. DIM. ±.005 / ±.010 / ±.015					
FRACT. DIM. ± 1/64 / ± 1/32 / ± 1/16	FINISH	ISSUED	USED WITH	AP'PD	DWN.
UNLESS OTHERWISE SPECIFIED					

Federal Telecommunication Laboratories, Inc. -1

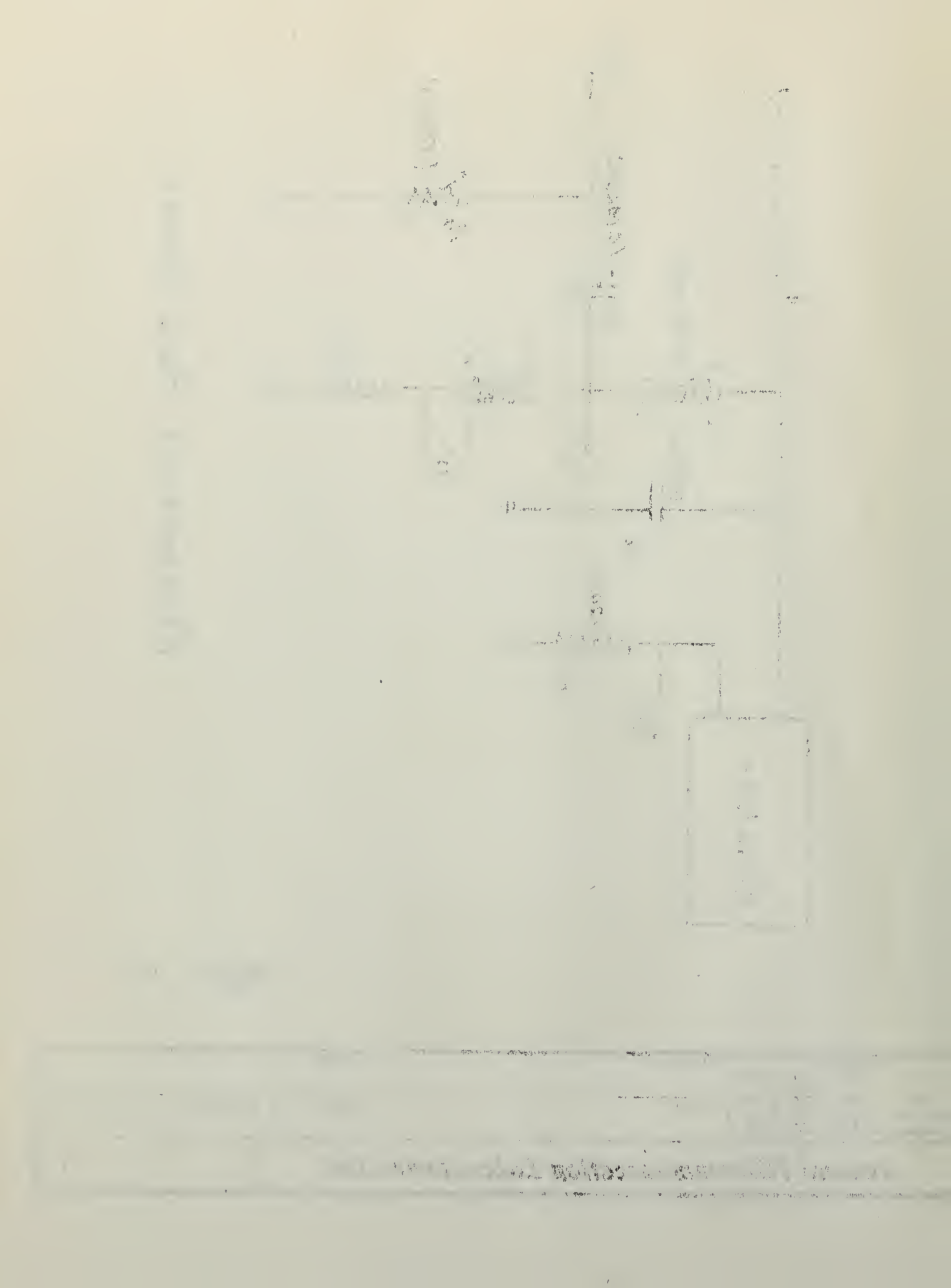

(a) Point "A"

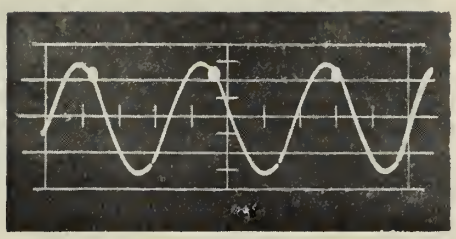

Input voltage, 60v rms; CRT cathode modulated by + and − output pulses.

(b) Point "B"

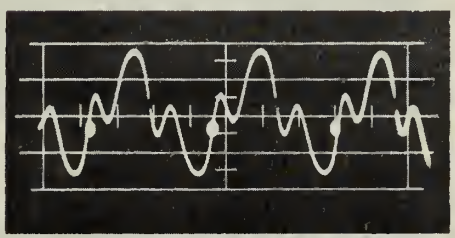

Input current, 1.8ma rms, 3.0ma peak; CRT cathode modulated.

(c) Point "C"

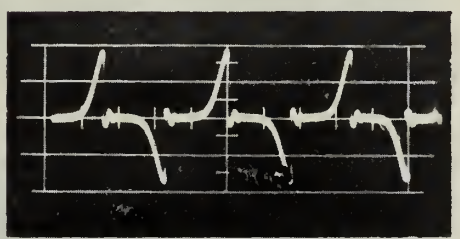

Voltage across saturable core reactor, 75v peak.

(d) Point "D"

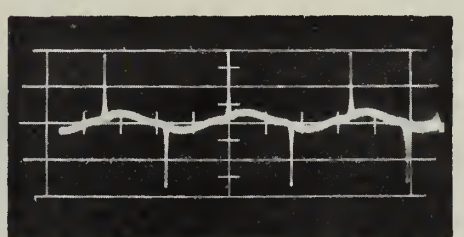

Current through reactor, 7.1ma rms, 95ma peak.

FIGURE 20

REGENERATIVE PULSE FORMER; TYPICAL WAVEFORMS

(a) Point "E"

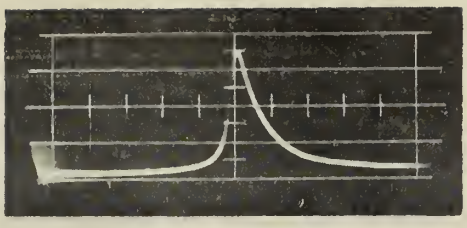

Output voltage, 60v peak.

(b) Point "E"

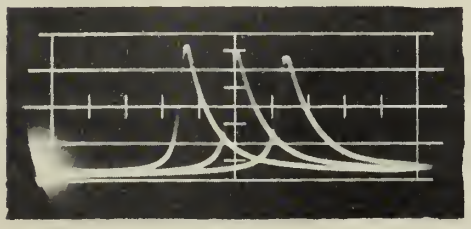

Phase shift with 10% variation of tuning inductance;
L_1 = 330mh, 370mh, 410mh.

c) Point "E"

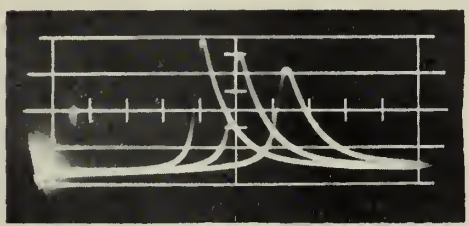

Phase shift with 10% variation of input voltage;
e_{in} = 66v, 60v, 54v.

(d) Point "E"

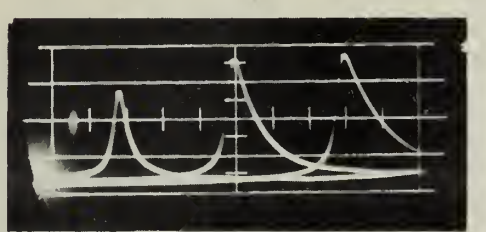

Phase shift with variation of peaking capacitance;
C_2 = 0.001μf, 0.002μf, 0.003μf.

(e) Point "E"

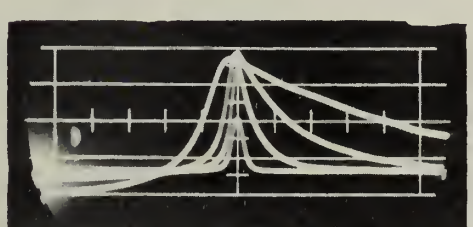

Change of pulse shape with variation of output resistance.
R_2 = 100Ω, 500Ω, 1500Ω, 5000Ω.

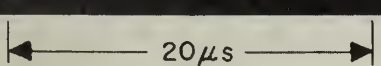

FIGURE 21
REGENERATIVE PULSE FORMER; OUTPUT WAVEFORMS

59. It is anticipated that an all-around improvement of the circuit behavior may be achieved by the use of Supermalloy cores of smaller dimensions. Small diameter cores of from 5 to 50 turns of 1-mil tape will probably prove to be most suitable. These cores should require windings of 1500 to 300 turns correspondingly. The smaller cores are on order and will be available for test in the near future.

60. Figure 22 shows photographs of a pulse former similar to the one tested. Its size and weight are considerably larger than necessary; in particular, the cores of the two toroidal coils used could be reduced in size appreciably. In its production form the unit will be potted to avoid corrosion of the coil windings. In this condition it will have indefinite life expectancy and nearly complete freedom from the effects of shock and vibration accelerations.

IV. MAGNETIC COINCIDENCE GATES

61. Only a small proportion of the work was devoted to study of magnetic coincidence gates. The following paragraphs cover the theory of operation of such a device and the design of a pulse-generating circuit for testing magnetic cores for use in the gate.

A. Basic Operation

62. A schematic of the core unit to be employed is shown in Figure 23. Coils 1 and 2 are the input coils; the output appears across coil 3.

63. The following discussion of the operation of a magnetic gate may best be understood by close reference to Figure 24. The typical loop of part (a) has been idealized for ease of discussion in part (b).

64. The symbols used are defined as follows:

H_1 - magnetizing force due to current signal in coil 1

H_2 - magnetizing force due to current signal in coil 2

FIGURE 22
REGENERATIVE PULSE FORMER

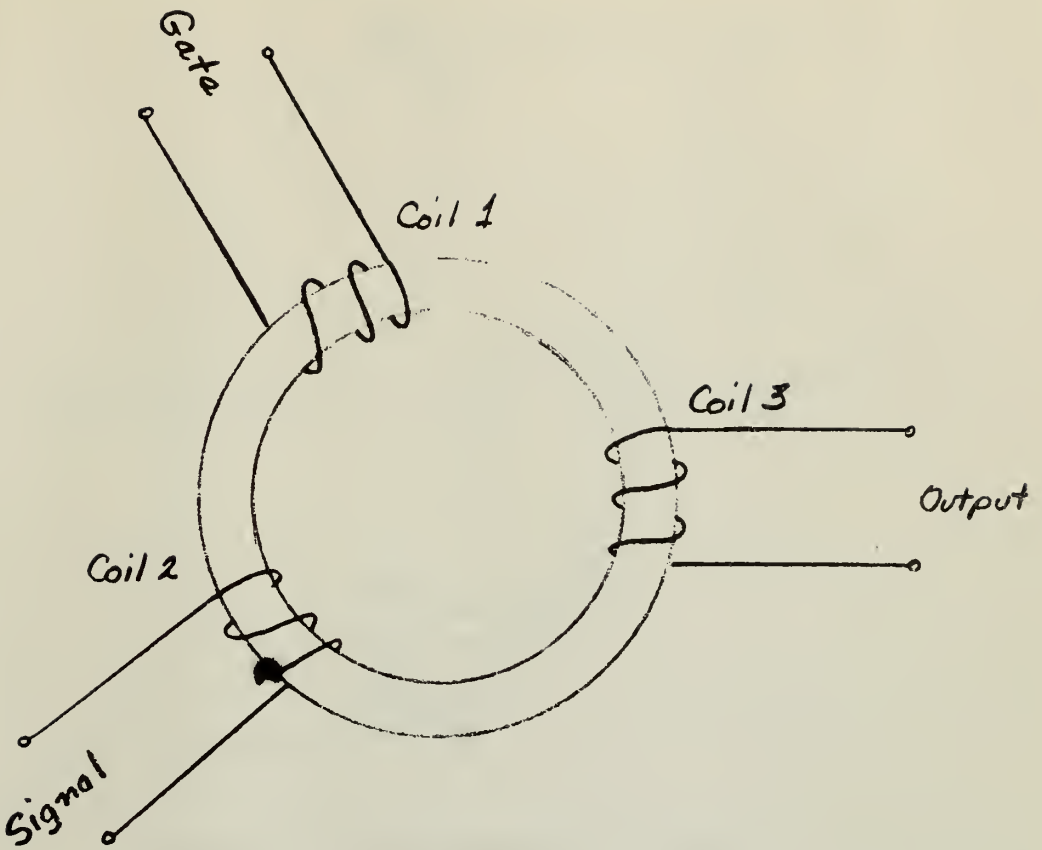

COINCIDENCE GATE SCHEMATIC

Figure 23

TOLERANCE	MATERIAL	TITLE			
UP TO 6 / ABOVE 6 TO 24 / ABOVE 24					
DEC. DIM. ±.005 / ±.010 / ±.015	FINISH	ISSUED	USED WITH	AP'PD	DWN.
FRACT. DIM. ± 1/64 / ± 1/32 / ± 1/16					
UNLESS OTHERWISE SPECIFIED					

Federal Telecommunication Laboratories, Inc. -1

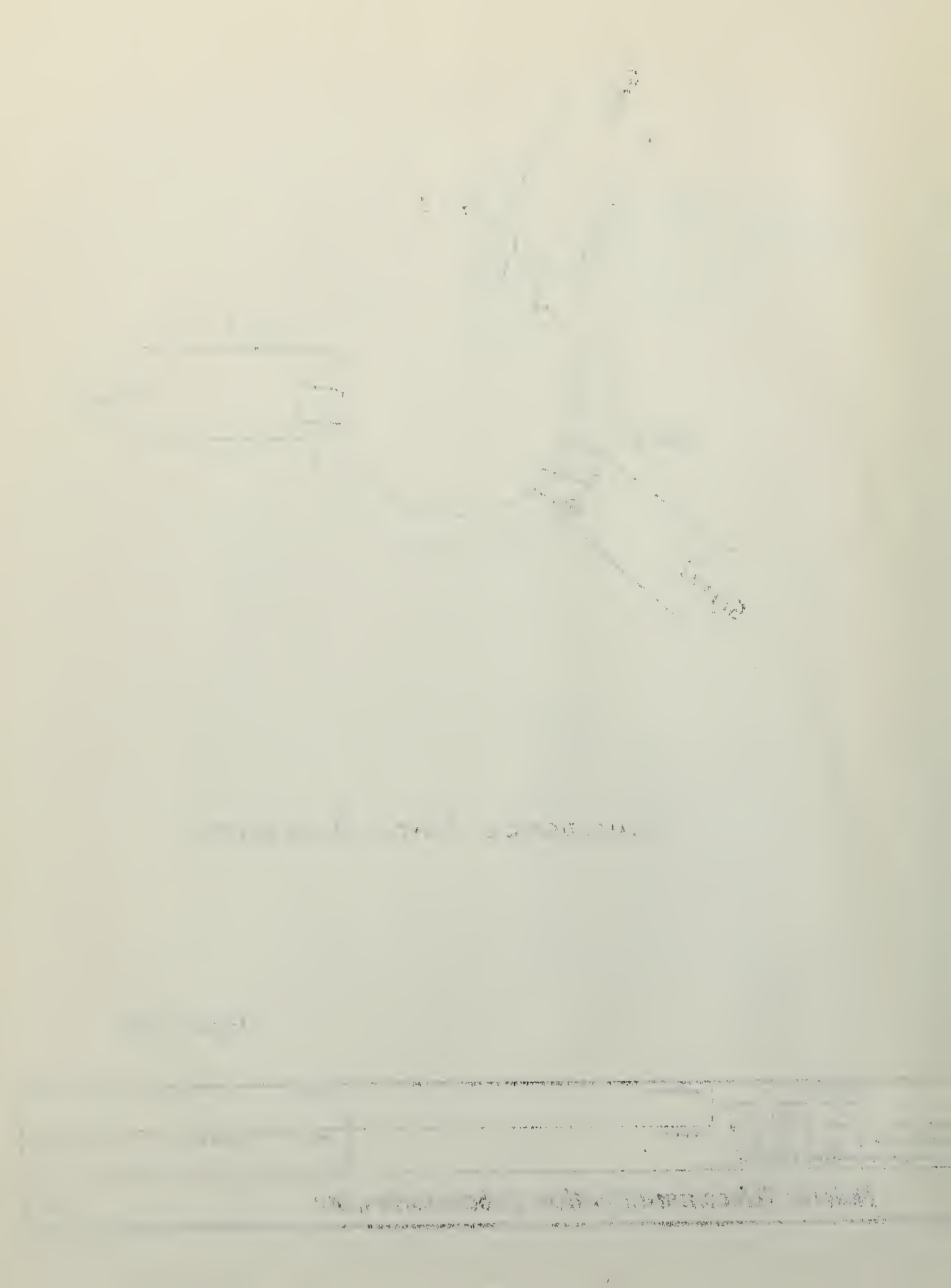

(a)

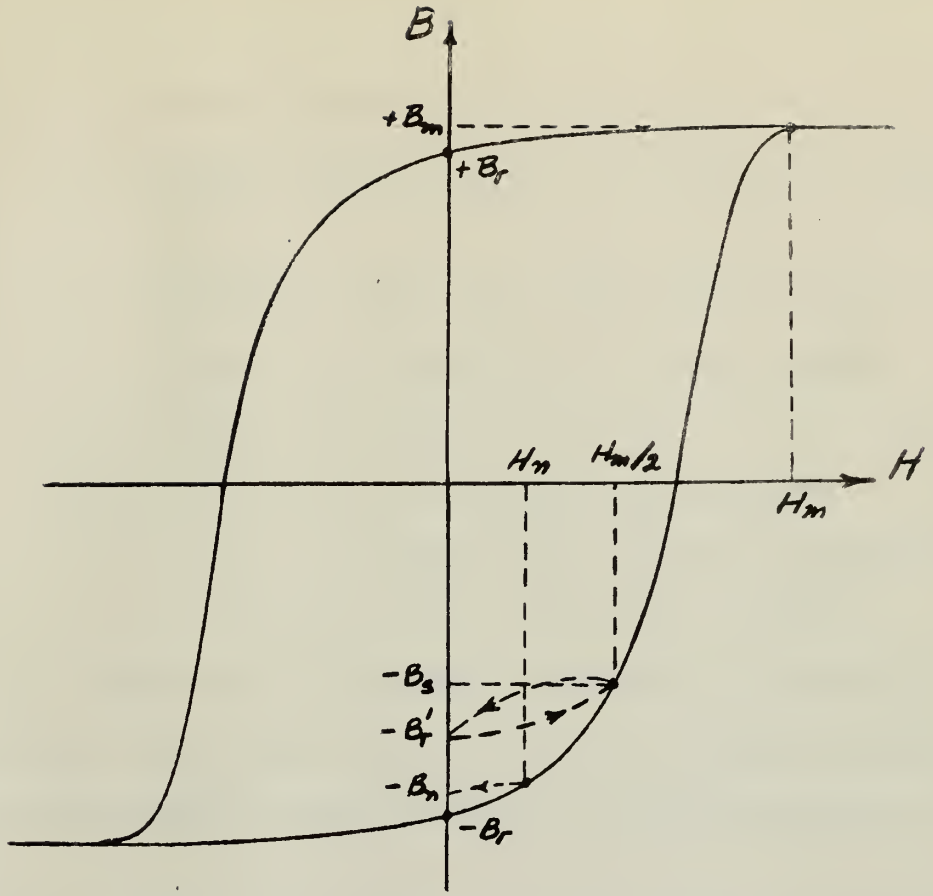

TYPICAL HYSTERESIS LOOP

(b)

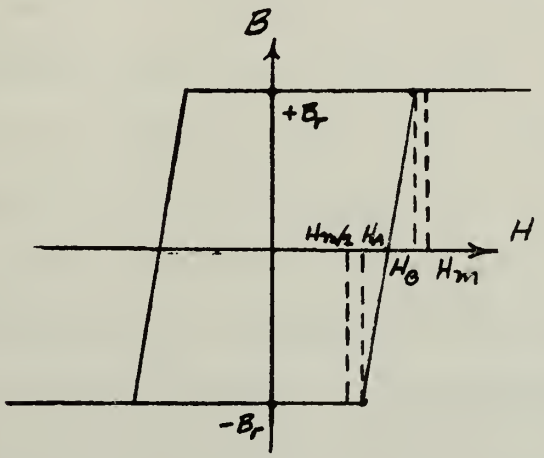

IDEALIZED HYSTERESIS LOOP

Figure 24

TOLERANCE				MATERIAL	TITLE			
	UP TO 6	ABOVE 6 TO 24	ABOVE 24					
DEC. DIM.	±.005	±.010	±.015					
FRACT. DIM.	± 1/64	± 1/32	± 1/16	FINISH	ISSUED	USED WITH	AP'PD	DWN.
UNLESS OTHERWISE SPECIFIED								
Federal Telecommunication Laboratories, Inc.								-1

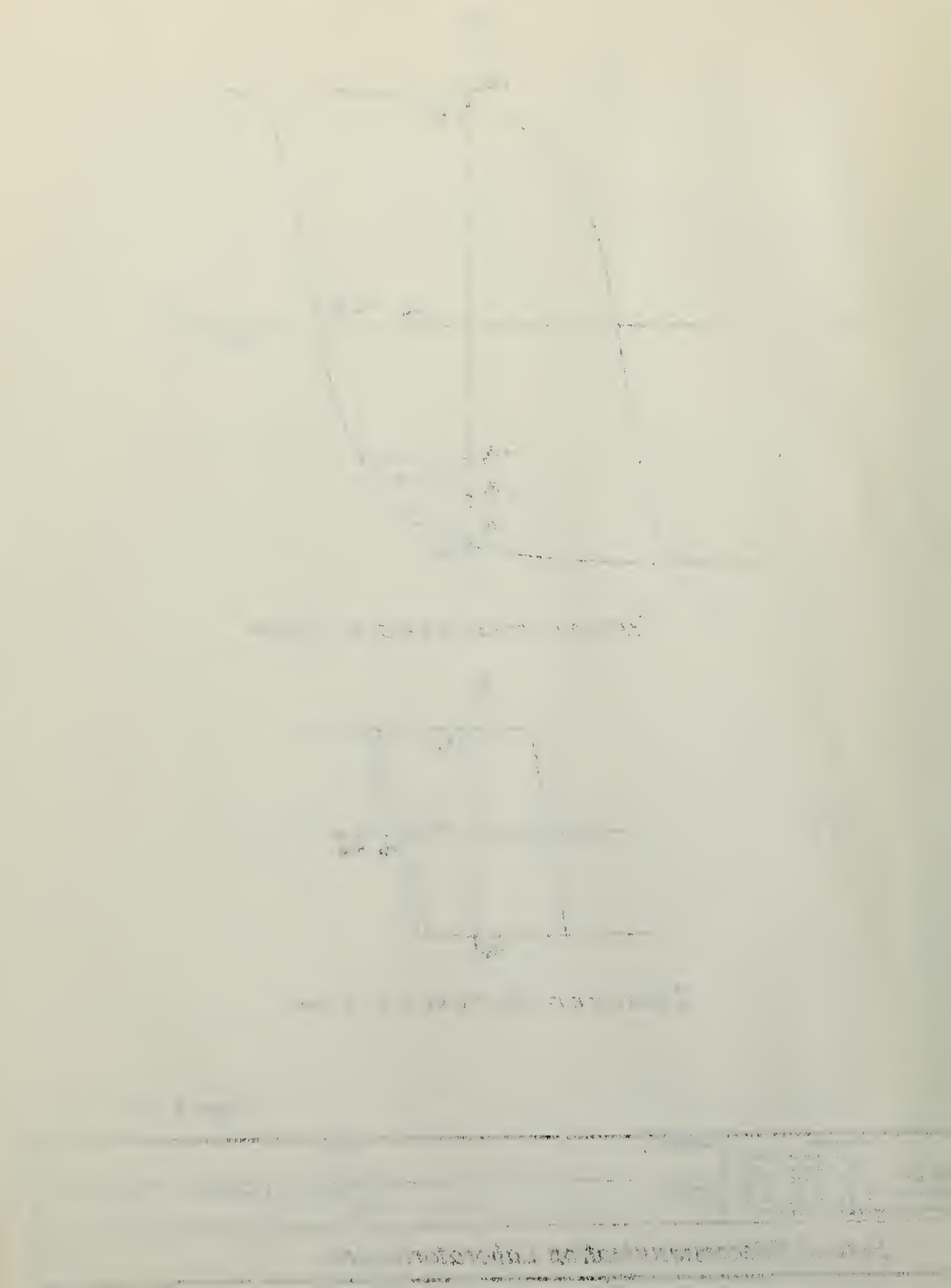

H_m - maximum magnetizing force ($H_1 + H_2$)

H_d - negative magnetizing force to return core to operating point

H_n - magnetizing force due to noise signals in coil 1 or coil 2

B_r - residual flux density with excitation removed

B_m - maximum flux density

B_s - flux density during single-coil excitation

B_r' - residual flux density after single-coil excitation

B_n - residual flux density after noise excitation

65. Referring to Figure 24(a), assume that the operating point is at the lower stable position $-B_r$. This may be achieved by arranging to introduce large negative H pulses between the information-carrying positive signals.

66. Assuming $H_1 = H_2 = H_m/2$, the application of a signal to one of the input coils results in a relatively minor change of flux density from $-B_r$ to $-B_s$ and a correspondingly small output signal. Upon removal of the input signal, the core flux density goes to $-B_r'$, from which it is returned to $-B_r$ by the negative restoring pulse, H_d.

67. If signals are applied to coils 1 and 2 simultaneously, the core reverses its magnetization in proceeding to the $+B_m$ condition. The large change of flux density results in a correspondingly large output signal. This is essentially the operation of the magnetic coincidence gate.

68. Noise signals result in changing the operating point from $-B_r$ to $-B_n$. This change is not likely to present any serious difficulty unless noise conditions are unusually adverse.

69. In actual operation the gating pulse and the negative restoring pulse might be applied to one winding and the signal pulse to the other. Then only if the gating pulse and signal pulse are coincident in time will an appreciable positive output pulse occur.

70. Two simple operating criteria may be derived from the idealized loop of Figure 24 (b). If the loop corner values of H are H_A and H_B as shown, the following must hold for coincidence operation:

$$H_m > H_B$$

$$H_m/2 < H_A$$

(1) $$2H_A > H_m > H_B$$

(2) $$|H_d| > H_m$$

71. For ideal operation the hysteresis loop should be rectangular, that is, H_A should equal H_B; but in any case the loop must have the following characteristic:

(3) $$H_B < 2H_A$$

72. The present literature indicates that, because of the fast response time previously discussed in Paragraph 15, the ferritic-type cores alone are suitable for the proposed gates. Of these, the Ferramic A-34 cores, which are not available at the present time because of difficulties in processing, seem to be the most promising.

B. Test Circuit

73. A test setup for investigating the characteristics of magnetic cores for coincidence-gate operation is shown in Figure 25. The dotted block encloses a pulse-generating circuit capable of producing the negative restoring pulse, positive gating pulse, and positive signal pulse in proper synchronization.

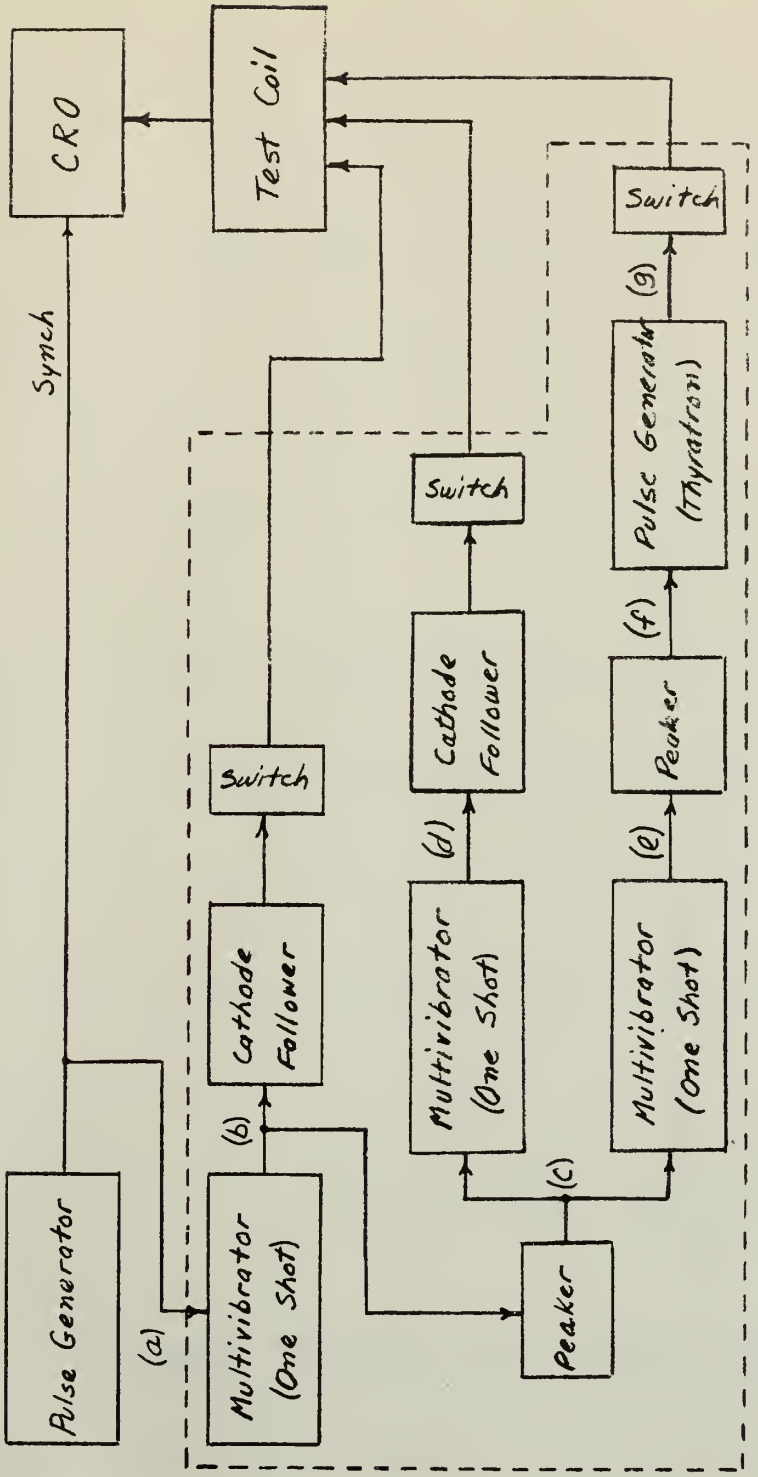

COINCIDENCE GATE TEST ARRANGEMENT

Figure 25

TOLERANCE				MATERIAL	TITLE			
	UP TO 6	ABOVE 6 TO 24	ABOVE 24					
DEC. DIM.	±.005	±.010	±.015					
FRACT. DIM.	± 1/64	± 1/32	± 1/16	FINISH	ISSUED	USED WITH	AP'PD	DWN.
UNLESS OTHERWISE SPECIFIED								

Federal Telecommunication Laboratories, Inc. -1

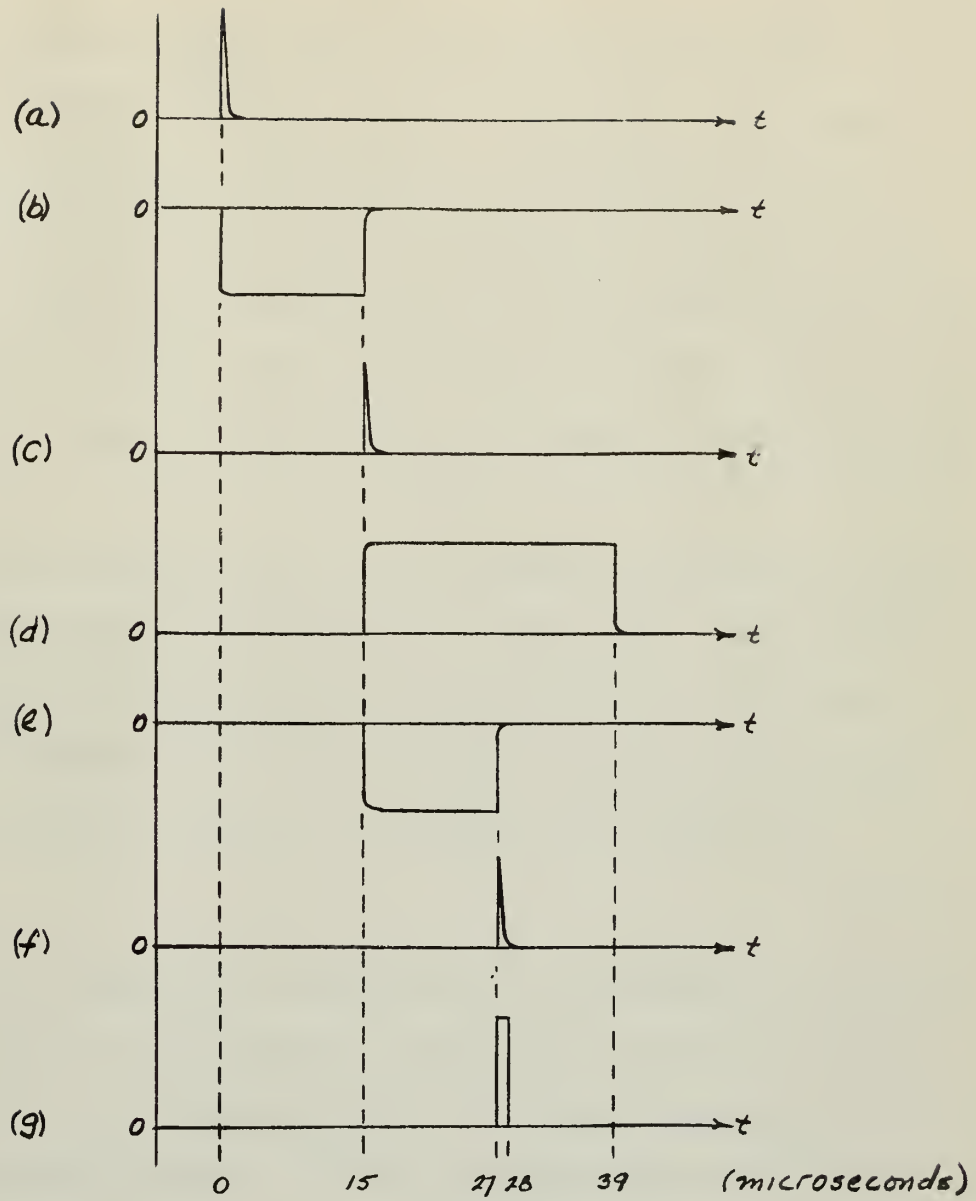

WAVE FORMS OF FIGURE 25

Figure 26

TOLERANCE				MATERIAL	TITLE			
	UP TO 6	ABOVE 6 TO 24	ABOVE 24					
DEC. DIM.	±.005	±.010	±.015					
FRACT. DIM.	± 1/64	± 1/32	± 1/16	FINISH	ISSUED	USED WITH	AP'PD	DWN.
UNLESS OTHERWISE SPECIFIED								
Federal Telecommunication Laboratories, Inc.								-1

Figure 26 shows the voltage wave forms occurring in the test setup.

74. The detailed circuitry of the test circuit in the dotted block is shown in Figure 27. The first cathode-coupled multivibrator, V_1, produces the negative restoring pulse and triggers two other similar multivibrators. The second multivibrator, V_2, produces the positive gating pulse, which is applied to the same winding as the restoring pulse. Stage V_3 functions as a time delay to trigger the thyratron, V_6, at some time during the gating pulse.

75. The time duration of the multivibrator outputs may be varied by adjusting the positive bias levels of their input grids. The generated pulse amplitudes may be controlled by the potentiometers in the cathode circuits of the thyratron and cathode followers, V_4 and V_5. The switches permit any combination of pulses to be impressed on the test coil.

V. CONCLUSION

76. The regenerative magnetic pulse former designed and built is considered superior to its vacuum-tube counterpart in nearly all respects. It is not limited to use in the application for which designed, but may be adapted for many other purposes. In fact, under slightly less rigorous phase-stability requirements, it may be simplified considerably by the substitution of a resistor for the input resonant circuit.

77. The following is a ~~brief~~ ie discussion of the important general characteristics of the regenerative pulse former.

A. Weight

Because of the successful subminiaturization of vacuum tubes and their components, the absolute weight reduction is not great for each unit. However, considering that several units will be used in the equipment and that

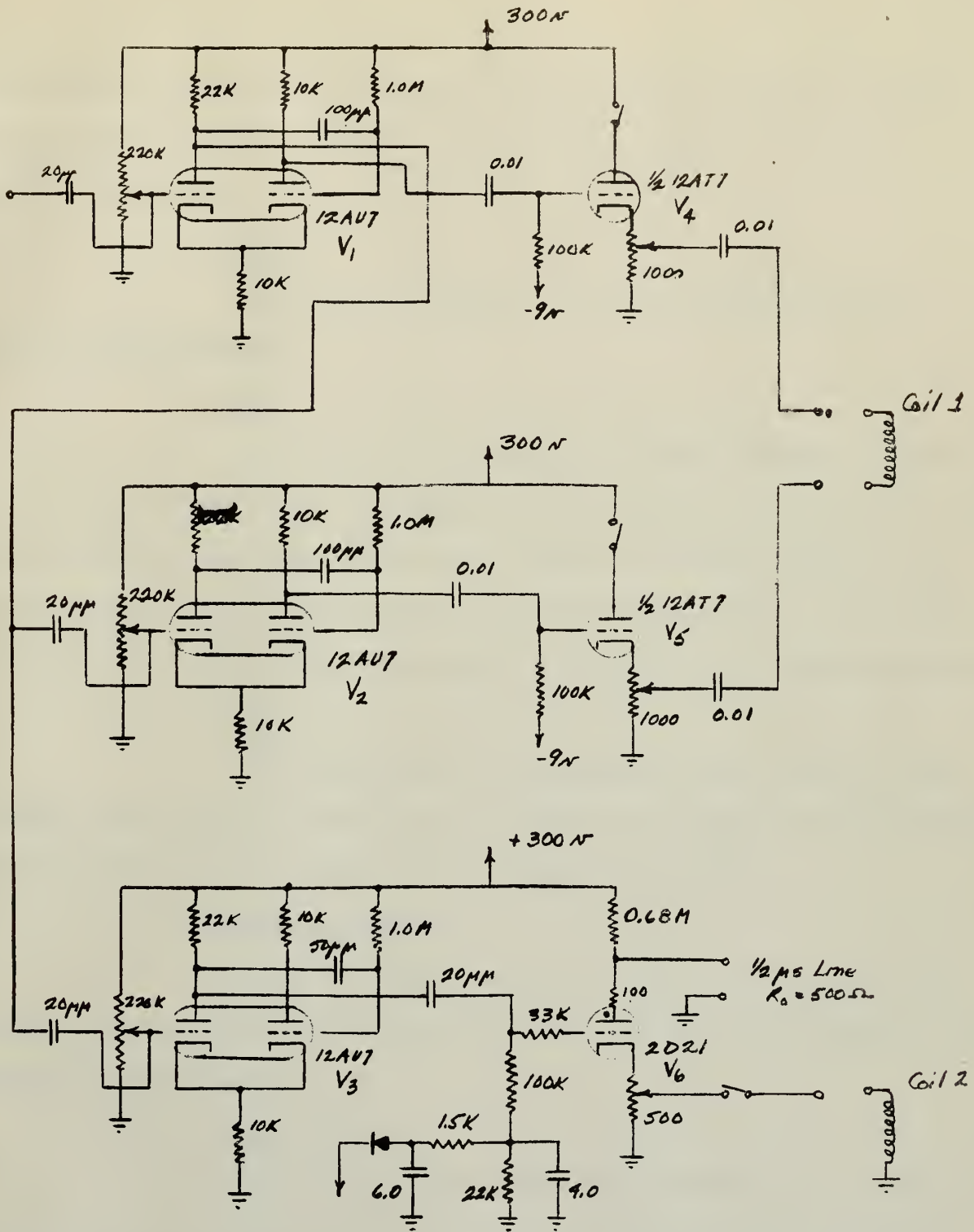

PULSE GENERATOR CIRCUIT

Figure 27

TOLERANCE	MATERIAL	TITLE			
UP TO 6 / ABOVE 6 TO 24 / ABOVE 24					
DEC. DIM. ±.005 / ±.010 / ±.015					
FRACT. DIM. ± 1/64 / ± 1/32 / ± 1/16	FINISH	ISSUED	USED WITH	AP'PD	DWN.
UNLESS OTHERWISE SPECIFIED					

Federal Telecommunication Laboratories, Inc. -1

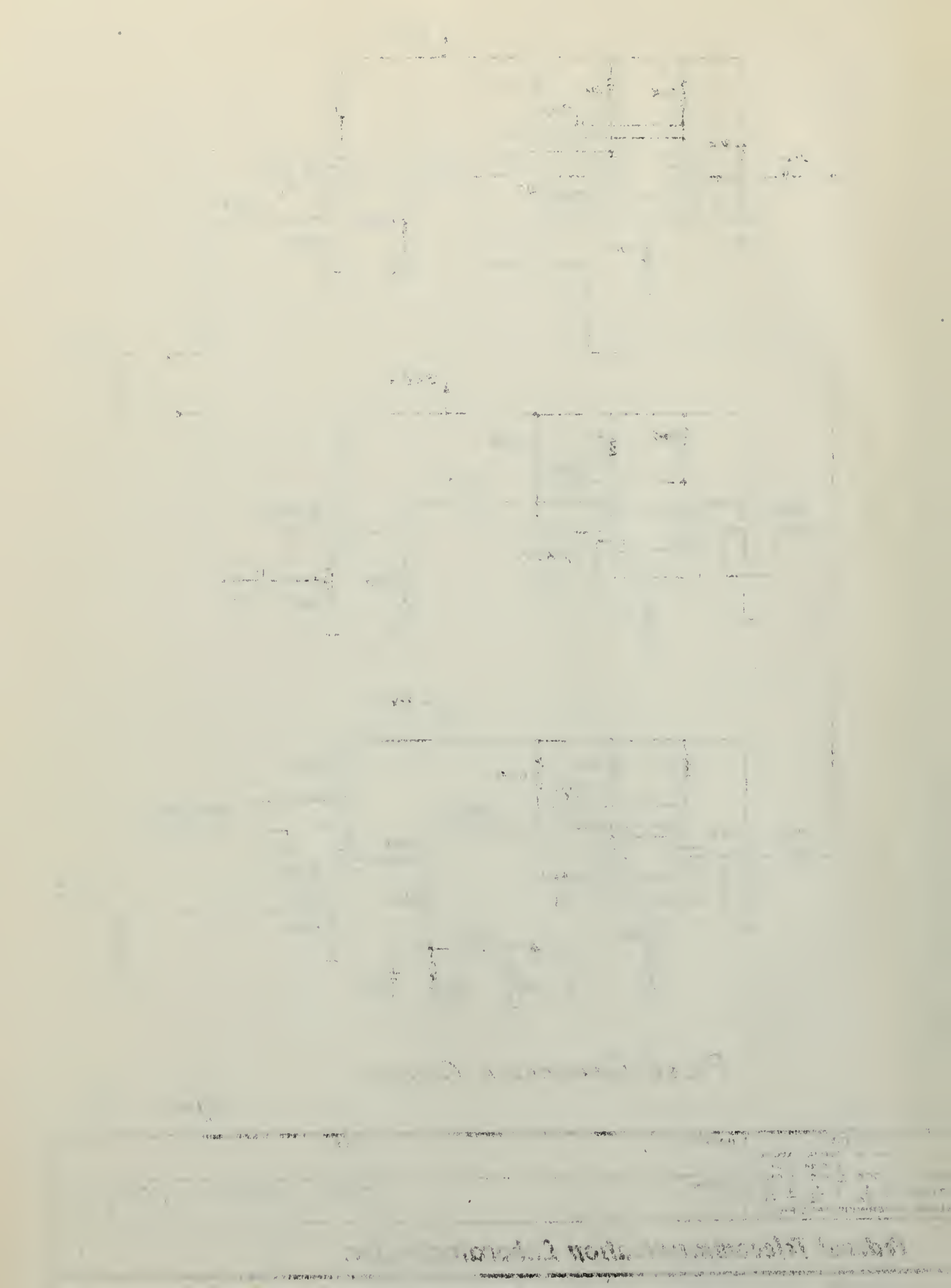

the aircraft manufacturers' criterion is eight pounds of airframe for each one pound of electronic equipment, it is apparent that the reduction in weight is important.

B. Volume

Comparison of Figures 2 and 22 indicates the large saving of space achieved.

C. Heat

In view of the heat-removal problems presented by modern high-altitude aircraft, heat and temperature are important considerations. The heat generated in the regenerative pulse former due to power dissipation is approximately 0.1 watt, probably less than the filament power in the vacuum-tube circuit and several times less than the latter's over-all power dissipation.

D. Power

A disadvantage of the regenerative pulse former is that it draws power from its driving source. However, the vacuum-tube pulse former requires many times more power from the primary power supply.

E. Impedance Levels

Since the input impedance is fairly high (33,000 ohms), excitation of the device presents few problems. The low output impedance (500 ohms) is also advantageous.

F. Reliability

Probably the greatest advantage offered by the regenerative pulse former is its reliability. It has theoretically infinite life and is inherently extremely rugged.

G. Cost

Last but not the least of its advantages is the low cost of the regenerative pulse formers as compared with that of the vacuum-tube circuit it replaces.

APPENDIX A

QUANTITATIVE ANALYSIS OF PERFORMANCE OF PEAKING TRANSFORMER WITH SHUNT

a. In the following development the subscripts have the below-listed connotation:

p, A - primary core (Hipersil)

s, B - secondary core (Supermalloy)

sh, C - shunt core (Hipersil)

gA - air gap between A and B due to surface irregularities

gC - gap between C and B

The prime (') superscript indicates saturation values.

b. The physical constants of the core are as follows:

$A_p = 0.725 \text{ cm}^2$

$\ell_p = 10.25$ cm (includes shunt path)

$N_p = 1000$ turns

$A_s = 0.00161 \text{ cm}^2$

$\ell_s = 1.27$ cm

$N_s = 400$ turns

$A_g = 0.806 \text{ cm}^2$

$\ell_{gA} = 0.00254$ cm

$\ell_{gC} = 0.0254$ cm

c. Assume a driving voltage of 70 volts rms and a current of 14 milliamperes rms (0.98 volt-amperes). Then the peak magnetizing force, H_{max}, is

$$H_{max} = \frac{0.4 \pi N_p I_{max}}{\ell_p}$$

= 2.42 oersteds

Referring to Figure 6, $B_s' = 5700$ gauss and $H_s' = 0.30$ oersteds, from which the average permeability, $\bar{\mu}_s$, in the unsaturated region is

$$\bar{\mu}_s = \frac{B_s'}{H_s'}$$

$$= 19{,}000$$

d. Neglecting leakage flux, the simple equivalent magnetic circuit shown in Figure 28 may be drawn. From the formula $\mathcal{R} = \ell/\mu A$, when the secondary core is unsaturated,

$$\mathcal{R}_A = \mathcal{R}_C = 0.000236$$

$$\mathcal{R}_B = 0.0716$$

$$\mathcal{R}_{gA} = 0.00315$$

$$\mathcal{R}_{gC} = 0.0315$$

Thus at least 70 percent of the available magnetomotive force is used to saturate the secondary core. Increasing the air gap would improve this figure somewhat.

e. Assuming the permeability of the Hipersil to be 25,000, the inductance, L, during saturation is

$$L = \frac{4\pi N_p^2 A_p \times 10^{-8}}{\ell_g + \ell_C/\mu}$$

$$= 0.344 \text{ henrys}$$

For the assumed 70 volts input, the actual current may now be computed.

$$i_{in} = \frac{e_{in}}{2\pi f L}$$

$$= 12.0 \text{ milliamperes}$$

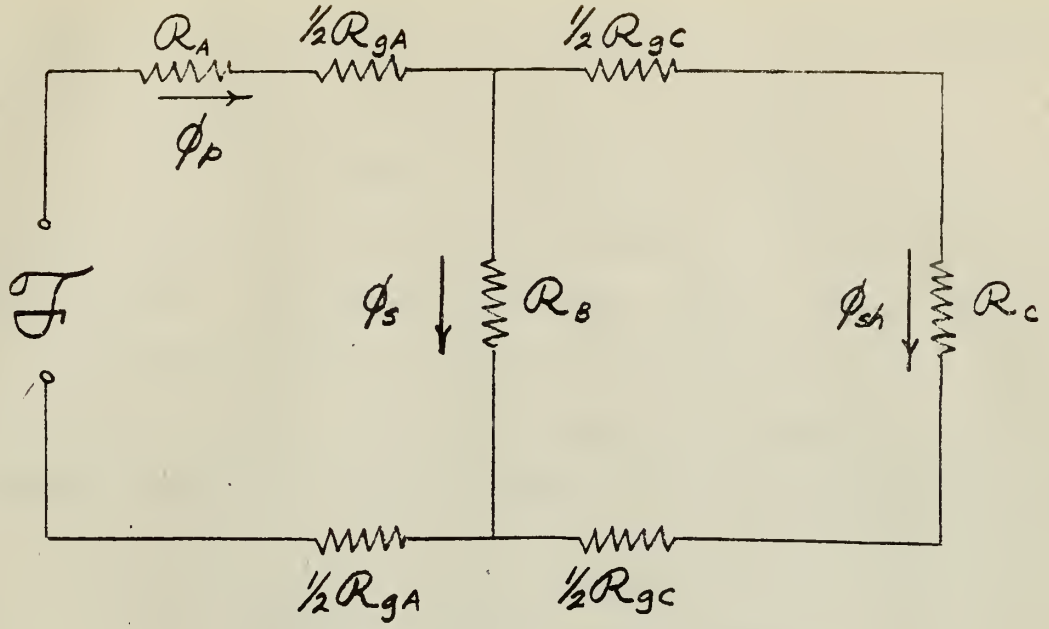

EQUIVALENT MAGNETIC CIRCUIT

PEAKING TRANSFORMER WITH SHUNT

Figure 28

TOLERANCE	MATERIAL	TITLE			
UP TO 6 / ABOVE 6 TO 24 / ABOVE 24					
DEC. DIM. ±.005 / ±.010 / ±.015	FINISH	ISSUED	USED WITH	AP'PD	DWN.
FRACT. DIM. ± 1/64 / ± 1/32 / ± 1/16					
UNLESS OTHERWISE SPECIFIED					
Federal Telecommunication Laboratories, Inc.					-1

Since this is reasonably close to the assumed current of 14 milliamperes; no correction of the foregoing work is considered necessary.

g. Now referring to the graph of Figure 11, with a peak magnetizing force of 2.42 oersteds the hysteresis loop width is 14 microseconds. Figure 6 indicates that the rate of change of flux varies from zero to its maximum value during a change of magnetizing force of approximately 0.4 times the loop width. The output voltage thus reaches its peak in 5.6 microseconds. The maximum rate of change of flux as determined from Figure 6 is

$$\frac{d \phi_s}{dt} = 3.3 \times 10^6 \text{ maxwells/second}$$

From the relation $e = N \frac{d\phi}{dt} \times 10^{-8}$, the maximum output voltage is computed to be 13.2 volts.

h. These calculations predict an output pulse of the following characteristics:

Pulse Amplitude	13.2 volts
Pulse Rise Time	5.6 microseconds

REFERENCE BIBLIOGRAPHY

1. William N. Papian; "A Coincident-Current Magnetic Memory Unit," Report 192, Servomechanisms Laboratory M.I.T., Sept. 8, 1950.

2. James C. Miles; "Saturable-Core Reactors as Digital Computer Elements," Engineering Research Associates, Inc., Contract NObsr-42001, June 17, 1949.

3. H. B. Rex, "Bibliography on Transducers, Magnetic Amplifiers, etc.," Instruments, Vol. 21, April, 1948.

4. J. H. Crede and J. P. Martin, "Magnetic Characteristics of an Oriented 50% Nickel-Iron Alloy," Journal of Applied Physics, Vol. 20, No. 10, pp 966-971, October, 1949.

5. A. G. Ganz; "Applications of Thin Permalloy-Tape Magnetic Amplifiers and Pulse Transformers," Electrical Engineering (Transactions Section), Vol. 65, pp 177-183, April, 1946.

6. "Symposium of Papers on Ferromagnetic Materials," Institution of Electrical Engineers, Vol. 97, Part II, No. 56, April, 1950.

7. G. N. Glasoe and J. V. Lebacqz; "Pulse Generators," McGraw-Hill Book Co., 1948.

8. Leonard R. Crow; "Saturating Core Devices," Scientific Book Publishing Co., 1949.

9. Richard M. Boyorth; "Ferromagnetism," D. Van Nostrand Co., Inc., 1951.

10. Reuben Lee; "Electronic Transformers and Circuits," John Wiley and Sons, Inc., 1947.

11. A. S. Langsdorf; "Principles of Direct-Current Machines," McGraw-Hill Book Co., Inc., 1940.

12. E. Peterson; "Coil Pulsers for Radar," Bell System Technical Journal, Vol. 25, pp 603-615, October, 1946.

13. E. Peterson, J. M. Manley, L. R. Wrathall; "Magnetic Generation of a Group of Harmonics," Bell System Technical Journal, Vol. 16, pp 437-455, October, 1937.

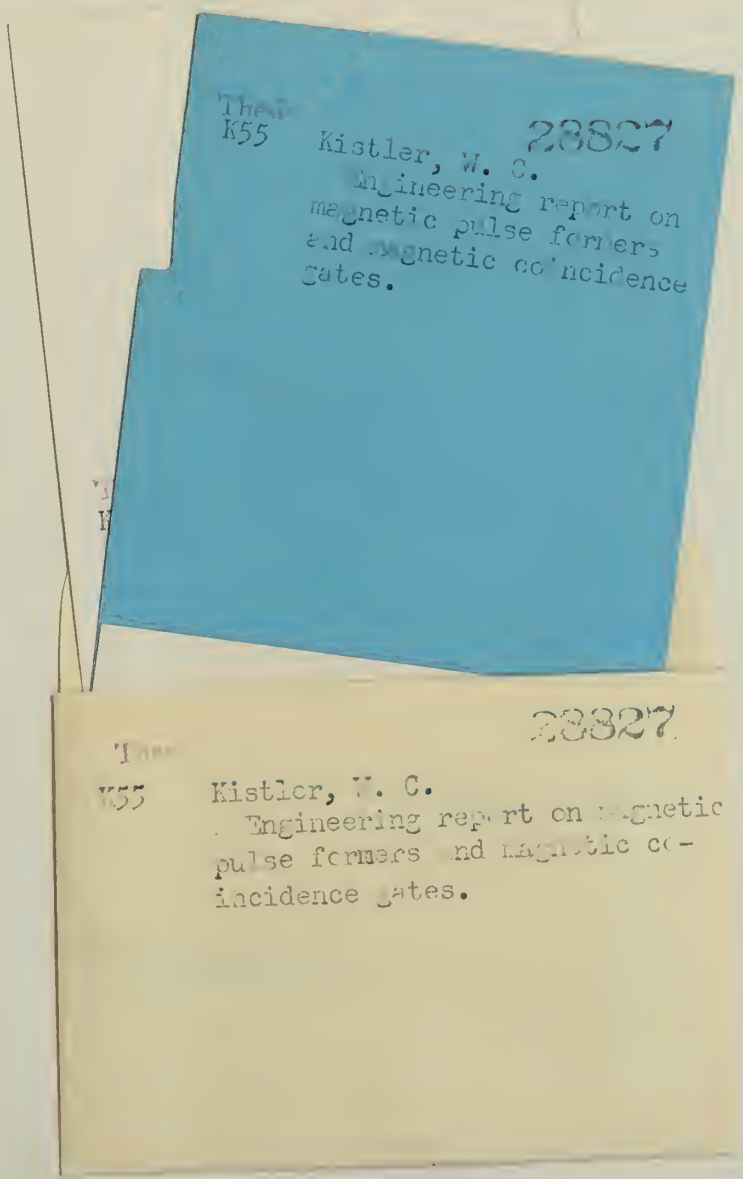

Thesis
K55 Kistler, W. C. 28827
Engineering report on magnetic pulse formers and magnetic coincidence gates.

28827
Thesis
K55 Kistler, W. C.
Engineering report on magnetic pulse formers and magnetic coincidence gates.